SLIDING MODE CONTROL OF LINEARLY ACTUATED NONLINEAR SYSTEMS

BURAK DURMAZ

JUNE 2009

SLIDING MODE CONTROL OF LINEARLY ACTUATED NONLINEAR SYSTEMS

A THESIS SUBMITTED TO
THE GRADUATE SCHOOL OF NATURAL AND APPLIED SCIENCES
OF
MIDDLE EAST TECHNICAL UNIVERSITY

BY

BURAK DURMAZ

IN PARTIAL FULFILLMENT OF THE REQUIREMENTS
FOR
THE DEGREE OF MASTER OF SCIENCE
IN
MECHANICAL ENGINEERING

JUNE 2009

Approval of the thesis:

SLIDING MODE CONTROL OF
LINEARLY ACTUATED NONLINEAR SYSTEMS

submitted by **BURAK DURMAZ** in partial fulfilment of the requirements for the degree of **Master of Science in Mechanical Engineering Department, Middle East Technical University** by,

Prof. Dr. Canan Özgen ----------
Dean, Graduate School of **Natural and Applied Sciences**

Prof. Dr. Suha Oral ----------
Head of Department, **Mechanical Engineering**

Prof. Dr. M. Kemal Özgören ----------
Supervisor, **Mechanical Engineering Dept., METU**

Assoc. Prof. Dr. Metin U. Salamcı ----------
Co-Supervisor, **Mechanical Engineering Dept., Gazi University**

Examining Committee Members:

Prof. Dr. Y. Samim Ünlüsoy ----------
Mechanical Engineering Dept., METU

Prof. Dr. M. Kemal Özgören ----------
Supervisor, Mechanical Engineering Dept., METU

Prof. Dr. Bülent E. Platin ----------
Mechanical Engineering Dept., METU

Prof. Dr. Yücel Ercan ----------
Mechanical Engineering Dept., TOBB ETU

Assoc. Prof. Dr. Metin U. Salamcı ----------
Mechanical Engineering Dept., Gazi University

Date: 04 June 2009

I hereby declare that all information in this document has been obtained and presented in accordance with academic rules and ethical conduct. I also declare that, as required by these rules and conduct, I have fully cited and referenced all material and results that are not original to this work.

Name, Last name: Burak DURMAZ

Signature :

ABSTRACT

SLIDING MODE CONTROL OF
LINEARLY ACTUATED NONLINEAR SYSTEMS

Durmaz, Burak
Ms.C., Department of Mechanical Engineering
Supervisor : Prof. Dr. M. Kemal Özgören
Co-Supervisor : Assoc. Prof. Dr. Metin U. Salamcı

June 2009, 123 pages

This study covers the sliding mode control design for a class of nonlinear systems, where the control input affects the state of the system linearly as described by $\dot{\mathbf{x}} = \mathbf{A}(\mathbf{x})\mathbf{x} + \mathbf{B}(\mathbf{x})\mathbf{u} + \mathbf{d}(\mathbf{x})$. The main streamline of the study is the sliding surface design for the system. Since there is no systematic way of designing sliding surfaces for nonlinear systems, a moving sliding surface is designed such that its parameters are determined in an adaptive manner to cope with the nonlinearities of the system. This adaptive manner includes only the automatic adaptation of the sliding surface by determining its parameters by means of solving the State Dependent Riccati Equations (SDRE) online during the control process. The two methods developed in this study: SDRE combined sliding control and the pure SDRE with bias terms are applied to a longitudinal model of a generic hypersonic air vehicle to compare the results.

Keywords: Sliding Mode Control, Variable Structure Control Systems (VSCS), State Dependent Riccati Equations (SDRE), Adaptive Control

ÖZ

DOĞRUSAL EYLETİMLİ DOĞRUSAL OLMAYAN SİSTEMLERİN KAYAN KİPLİ KONTROLU

Durmaz, Burak

Yüksek Lisans, Makina Mühendisliği Bölümü

Tez Yöneticisi : Prof. Dr. M. Kemal Özgören

Ortak Tez Yöneticisi: Doç. Dr. Metin U. Salamcı

Haziran 2009, 123 sayfa

Bu çalışma, durum değişkenleri kontrol girdilerince doğrusal olarak etkilenen doğrusal olmayan sistemler için kayan kipli kontrolcu tasarımını kapsamaktadır. Böyle bir sistem, $\dot{\mathbf{x}} = \mathbf{A}(\mathbf{x})\mathbf{x} + \mathbf{B}(\mathbf{x})\mathbf{u} + \mathbf{d}(\mathbf{x})$ biçiminde tanımlanabilir. Çalışmanın ana hattını, sistem için kayma yüzeyinin tasarlanması oluşturmaktadır. Doğrusal olmayan sistemler için sistematik bir kayma yüzeyi tasarlama yöntemi bulunmadığından bu çalışmada hareketli fakat parametreleri sistemin doğrusal olmayan özelliklerini etkisizleştirmek üzere sürekli uyarlanan bir kayma yüzeyi tasarlanmıştır. Buradaki uyarlama biçimi, kayma yüzeyi parametrelerinin Durum Bağımlı Riccati Denklemleri'nin (DBRD) kontrol süreci sırasında an be an çözülerek hesaplanmasını ve bu hesaplamalar kullanılarak yüzeyin otomatik olarak uyarlanmasını kapsamaktadır. Bu çalışmada geliştirilen iki yöntem: DBRD ile birleştirilmiş kayan kipli kontrolcü ve bias terimler içeren DBRD kontrol tasarımı hipersonik bir hava aracının boylamsal modeline uygulanmıştır.

Anahtar Kelimeler: Kayan Kipli Kontrol, Değişken Yapılı Kontrol Sistemleri, Durum Bağımlı Riccati Denklemleri, Uyarlamalı Kontrol.

To My Family

ACKNOWLEDGMENTS

The author wishes to express his deepest gratitude to his supervisor Prof. Dr. M. Kemal Özgören and co-supervisor Assoc. Prof. Dr. Metin U. Salamcı for their guidance, advice, criticism, encouragements and insight throughout the research.

The author also owes special thanks to his friend G. Serdar Tombul for his contributions and to his engineering leader in the company Burcu Özgör Demirkaya for her support and tolerance.

As a last word, the author is grateful to his family for their understanding, devotion and for the opportunities they provided.

TABLE OF CONTENTS

ABSTRACT.....ii

ÖZ.....iv

ACKNOWLEDGMENTS.....vii

TABLE OF CONTENTS.....viii

LIST OF FIGURES.....xi

LIST OF SYMBOLS.....xiv

CHAPTER

1. INTRODUCTION.....1

1.1 Sliding Mode Control.....1

1.2 Literature Survey.....4

1.3 Scope of the Thesis Study.....7

2. THEORATICAL BACKGROUND.....9

2.1 Introduction to SMC Design Technique.....9

2.1.1 Sliding Surfaces.....9

2.1.2 Controller Design.....15

2.1.3 Summary.....20

2.2 Methodology Used in This Study.....22

2.2.1 SMC Combined with SDRE (Adaptive Sliding Mode Control) 25

2.2.2 Pure SDRE Method.....48

3. APPLICATION OF THE DESIGNED CONTROLLER TO A HYPERSONIC AIR VEHICLE MODEL.....52

3.1 Mathematical Model of a Hypersonic Air Vehicle.....53

3.1.1 Nomenclature.....53

3.1.2 Differential Equations of the System.....55

3.2 Sliding Mode Control Design for the Hypersonic Air Vehicle Model.....58

3.3 Computer Simulations for the Designed Controller.....71

3.3.1 Simulations for the Case 1: Without Disturbance.....75

3.3.2 Simulations for the Case 2: With Disturbance.....84

4. CONCLUSIONS.....97

4.1 Summary.....97

4.2 Major Conclusions.....98

4.3 Recommendations for Future Work.....101

REFERENCES.....102

APPENDICES.....107

APPENDIX A MAIN SCRIPT.....107

APPENDIX B FUNCTION FOR DESIGNING CONTROLLER.....111

APPENDIX C FUNCTION FOR CONSTRUCTING SYSTEM AND CONTROL MATRICES.....115

APPENDIX D FUNCTION FOR TRANSFORMING THE SYSTEM TO CANONICAL FORM.....118

APPENDIX E FUNCTION FOR SLIDING SURFACE SLOPE DETERMINATION.....120

APPENDIX F BRIEF USER MANUAL.....122

VITA.....123

LIST OF FIGURES

FIGURES

Figure 2.1 Graphical interpretation of equations (2.2) and (2.4) (n=2).....13

Figure 2.2 Effect of **K** on the Chattering Phenomenon.....39

Figure 2.3 Typical SMC Input.....40

Figure 3.1 Free Body Diagram of a Simplified Hypersonic Air Vehicle.....55

Figure 3.2 Velocity Change.....76

Figure 3.3 Flight Path Angle.....76

Figure 3.4 Altitude Change.....77

Figure 3.5 Angle of Attack.....77

Figure 3.6 Pitch Rate.....78

Figure 3.7 Elevator Deflection.....78

Figure 3.8 Throttle Setting.....79

Figure 3.9 Variation of the Sigma Function – Deviation from Sliding Surface.....79

Figure 3.10 First and Second Sliding Surface Offset.....80

Figure 3.11 First and Second Components of the Sliding Surface Slope.....80

Figure 3.12 Third and Fourth Components of the Sliding Surface Slope.....81

Figure 3.13 Fifth and Sixth Components of the Sliding Surface Slope....81

Figure 3.14 First and Second Components of the Disturbance....82

Figure 3.15 Third and Fourth Components of the Disturbance....82

Figure 3.16 Fifth Component of the Disturbance and Delta Angle of Attack....83

Figure 3.17 Velocity Change....85

Figure 3.18 Flight Path Angle....85

Figure 3.19 Altitude Change....86

Figure 3.20 Angle of Attack....86

Figure 3.21 Pitch Rate....87

Figure 3.22 Elevator Deflection....87

Figure 3.23 Throttle Setting....88

Figure 3.24 Variation of the Sigma Function – Deviation from the Sliding Surface....88

Figure 3.25 First and Second Sliding Surface Offset....89

Figure 3.26 First and Second Components of the Sliding Surface Slope Slope....89

Figure 3.27 Third and Fourth Components of the Sliding Surface Slope....90

Figure 3.28 Fifth and Sixth Components of the Sliding Surface Slope....90

Figure 3.29 First and Second Components of the Transformed Disturbance....91

Figure 3.30 Third and Fourth Components of the Transformed Disturbance....91

Figure 3.31 Fifth Component of the Transformed Disturbance and Delta Angle of Attack.....92

Figure 3.32 Control Inputs for Integration Time Step is 0.1.....94

Figure 3.33 Control Inputs for Integration Time Step is 0.01.....95

Figure 3.34 Control Inputs for Integration Time Step is 0.001.....95

Figure 3.35 Control Inputs for Integration Time Step is 0.5.....96

LIST OF SYMBOLS

A	Speed of Sound
C_D	Drag Coefficient
C_L	Lift Coefficient
$C_M(q)$	Moment Coefficient due to Pitch Rate
$C_M(\alpha)$	Moment Coefficient due to Angle of Attack
$C_M(\delta_e)$	Moment Coefficient due to Elevator Deflection
C_T	Thrust Coefficient
C	Reference Length
D	Drag
h	Altitude
I_{yy}	Moment of Inertia
L	Lift
M	Mach Number
M_{yy}	Pitching Moment
m	Mass
q	Pitch Rate
R_E	Radius of the Earth
r	Radial Distance from Earth's Center
S	Reference Area
T	Thrust

V	Velocity
α	Angle of Attack
β	Throttle Setting
γ	Flight-Path Angle
δ_e	Elevator Deflection
μ	Gravitational Constant
ρ	Density of Air
ASMC	Adaptive Sliding Mode Control
LQR	Linear Quadratic Regulator
SMC	Sliding Mode Control
SDRE	State Dependent Riccati Equation

CHAPTER 1

INTRODUCTION

1.1 Sliding Mode Control

Variable Structure Control Systems (VSCS) evolved from the pioneering work of Emel'yanov and Barbashin in the early 1960s in Russia. The ideas did not appear outside of Russia until the mid 1970s when a book by Itkis and a survey paper by Utkin [1] are published in English. VSCS concepts have subsequently been utilised in the design of robust regulators, model-reference systems, adaptive schemes, tracking systems, state observers and fault detection schemes. The ideas have successfully been applied to problems as diverse as automatic flight control, control of electric motors, chemical processes, helicopter stability augmentation systems, space systems and robots. [2]

VSCS, as the name suggests, are a class of systems whereby the 'control law' is deliberately changed during the control process according to some defined rules which depend on the state of the system. Based on the concept of VSCS, the aim is to design a controller which will be sought to force the system states to reach, and subsequently remain on, a predefined surface within the state space.

The state space behaviour of the system is described as an ideal sliding motion when its state is confined to the surface. The advantages of obtaining such a motion are twofold: firstly, there is a reduction in the order of the dynamics which simplifies the controller design; secondly the sliding motion is insensitive to the matched uncertainties, which are the parameter variations and/or unknown inputs that occur in the same channels with the control inputs. This insensitivity at least against the matched uncertainties makes the methodology an attractive one for designing robust controllers for uncertain systems.

Model imprecision may come from actual uncertainty about the plant (e.g., unknown plant parameters), or from the purposeful choice of a simplified representation of the system's dynamics. Modelling inaccuracies can be classified into two major kinds: structured (or parametric) uncertainties and unstructured uncertainties (or unmodelled dynamics). The first kind corresponds to inaccuracies in the terms actually included in the model, while the second kind corresponds to the neglected higher order terms in the dynamic model.

Modelling inaccuracies can have strong adverse effects on nonlinear control systems. One of the most important approaches to dealing with model uncertainty is robust control. The typical structure of a robust controller is composed of a nominal part, similar to an ordinary feedback control law, and additional terms aimed at dealing with model uncertainty. Sliding Mode Control (SMC) technique is one of the important robust control approaches. For the class of systems to which it applies, SMC design provides a systematic approach to the problem of maintaining stability and consistent performance in the face of modelling imprecision.

Many different techniques have been developed for years to design sliding mode controllers. But the baselines of all different design techniques are very similar and consist of two main steps:

- Design the sliding (switching) surface in the state space so that the reduced-order sliding motion satisfies the specifications imposed by the designer,

- Determine the control law such that the trajectories of the closed-loop motion are directed towards the sliding surface and tried to be kept on the surface thereafter.

Discontinuity occurs due to the difference between the out-of-surface and surface-bound control laws. It can be avoided by replacing the sudden discontinuous switching between the two control laws with a rapid but continuous and gradual transition, such as using some kind of a saturation function instead of the sign function.

1.2 Literature Survey

As mentioned in Chapter 1.1, SMC design techniques are mainly developed after 1970s. Then, many studies have been done for the use of SMC technique both for linear and non-linear systems. Basically, research on SMC has recently developed in two main areas. The first is static SMC based on the works of DeCarlo et al. [3], Utkin [4] and Luk'yanov and Dodds [5]. The second approach is dynamic SMC which is based on differential (input-output) I-O systems, one of which is the work of Sira-Ramirez [6].

SMC is generally robust with respect to some kinds of uncertainties and modelling inaccuracies. For linear systems, the robustness property is well established. Robustness results also exist for particular types of non-linear systems. A general framework for the design of nonlinear sliding mode controllers based on the action of a one-parameter subgroup of diffeomorphisms on the sliding surface is represented in [7].

In most SMC schemes, the control laws usually utilise full-state feedback. In practice, this is not always possible, since the system states are not available or are expensive to measure. In case of so called immeasurable states, observer-based sliding mode controllers have been designed as studied in [8] by means of constructing an observer to estimate the unavailable states and then synthesising a SMC law based on the estimated states.

In addition to this, chattering phenomenon takes much more attraction in recent studies since it is thought that chattering is the only remaining obstacle in SMC design technique. Many design methods are proposed to overcome the effects of chattering.

There are many review papers on SMC. A recent one is prepared by K. David Young, Vadim I. Utkin and Ümit Özgüner in 1999 [9] which is a guide to summarise the basic design solutions and emphasise the effect of chattering phenomenon.

One of the recent trends on the SMC research is to combine the other control system design techniques with SMC. Within this context, the addition of adaptation capability to classical SMC may be considered as the combination of adaptive control and SMC. Furthermore, the addition of adaptation capability, named after as "Adaptive Sliding Mode Control (ASMC)", makes the sliding more sensible if it is thought that SMC is a subset of VSCS.

Some studies, which have been addressing the problem of designing adaptive sliding mode controllers for specific systems, can be found in the literature. In [10], adaptive sliding mode controller is designed for a hypersonic air vehicle model. In the study, firstly, the non-linear model of the hypersonic air vehicle is linearised by the application of input-output linearisation method. After that, two decoupled sliding surfaces are chosen based on the error dynamics. Errors are defined as the difference between the current velocity, altitude and the steady state (desired) values of the velocity and altitude respectively. Lastly, the sliding control design is accomplished by choosing control inputs such that the sliding conditions imply that the distance to the sliding surface decreases along all system trajectories are satisfied. Furthermore, the sliding condition makes the sliding surface an invariant set, i.e., once the system trajectories reach the surface, it will remain on it for the rest of the time. In addition, for any initial condition, the sliding surface is reached in a finite time.

In the work of Xu, H., et al [10], the sliding mode controller is combined with an on-line parameter estimator forming an adaptive sliding mode controller as well. The adaptive laws used to adapt the parameter estimations have been derived using the Lyapunov synthesis approach. The SMC alone and combined with the addition of an adaptive law (ASMC) techniques are simulated then accordingly under the presence of parametric uncertainty to see the advantages of the second method over the first one. As expected, a significant improvement in controller performance is observed. It is seen that the level of the control effort in the adaptive case is significantly smaller.

1.3 Scope of the Thesis Study

The main contribution of this study can be considered to be the addition of an adaptive manner to the SMC design for a state dependent and linearly actuated non-linear system. This is a contribution to the area of ASMC (Adaptive SMC) design, which is an attractive area for the researchers since it combines the power of SMC against uncertainties and disturbances with the ability of adapting the controller while the system is changing.

The technique used in [10] to design an ASMC for the hypersonic air vehicle model is explained in section 1.2. In this study, on the other hand, a different methodology has been developed to design the adaptive sliding mode controller for the same model used in [10]. First of all, the system is not linearised to design the sliding mode controller, in other words, the non-linearity of the original system is kept during the controller design phase. Secondly, the adaptation manner is added directly to SMC by means of adapting the slope of the sliding surface as well as its offset from the origin of the state space in accordance with the changes in the system state.

To make this adaptation, the so-called State Dependent Riccati Equations (SDRE) are solved while the state variables of the system are changing. Then the corresponding sliding surface slope and sliding surface offset are determined based on these calculations.

This technique not only turns the sliding mode controller to an adaptive one but it also allows to determine the slope and offset of the sliding surface optimally depending on the specified weighting matrices of a selected performance index.

The method can be outlined as follows (although a detailed explanation is given in section 2.2);

The system (represented by the state space formulation) is divided into two subsystems by using a state variable transformation such that all the control inputs are collected in the second subsystem while there remains no control input in the first subsystem, which is also called the reduced order system. Considering the first subsystem, the sliding surface is defined as a hyper surface in the state space based on two parameters: the sliding surface slope and the sliding surface offset. In this work, these parameters are determined optimally as functions of the state variables using the SDRE technique. The second subsystem, on the other hand, is used to determine the control inputs. The control inputs are determined to consist of two parts: the first part (known as *the nominal control*) is responsible of keeping the system state on the sliding surface and the second part (known as *the switching control*) is responsible of driving the system state toward the sliding surface whenever it is away from it.

CHAPTER 2

THEORETICAL BACKGROUND

2.1 Introduction to SMC Design Technique

Following three sections are mainly tailored from [11] to give brief information about the two main steps of the sliding mode control design.

2.1.1 Sliding Surfaces

This section analyses the Variable Structure Control (VSC) as a high-speed switched feedback control leading up to a sliding mode. For instance, each feedback path gains are switched between two values according to a rule that depends on the value of the system state at each instant. The purpose of the switching control law is to drive the state trajectory of the system onto a pre-specified (user-chosen) surface in the state space and to maintain the state trajectory on this surface for the subsequent time interval. This surface is called a switching surface. When the state trajectory is “above” the surface, the feedback controller uses one gain and a different gain if the state trajectory is “below” the surface. This surface defines the rule for a proper switching. This surface is also called a sliding surface (sliding manifold). [16]

Ideally, once intercepted, the switched control maintains the state trajectory on the surface forever and the state of the system slides on the surface toward the stable equilibrium point. The most important part is to design a switched control that drives the system state to the switching surface and keep it on the surface upon interception. A Lyapunov approach is used to carry out this task.

The Lyapunov method is usually used to determine the stability properties of an equilibrium point without solving the state equation. Let $V(\mathbf{x})$ be a continuously differentiable scalar function defined in a domain D that contains the origin. A function $V(\mathrm{x})$ is said to be positive definite if $V(0) = 0$ and $V(\mathrm{x}) > 0$ for $\|\mathbf{x}\| \neq 0$. It is said to be negative definite if $V(0) = 0$ and $V(\mathrm{x}) < 0$ for $\|\mathbf{x}\| \neq 0$. The Lyapunov method is to assure that the derivative of a properly defined positive definite function of the system state is negative definite. The function has a negative value when the function itself has a positive value and vice versa. Thus, the stability of the system is assured about the origin of the state space.

Lyapunov method, which was explained briefly above, is used to design the sliding mode controller. A candidate Lyapunov function, that characterises the motion of the system state to the sliding surface, is defined. For each chosen switched control structure, the "gains" are chosen such that the derivative of this Lyapunov function is negative definite, thus ensuring motion of the system state to the surface. After appropriate design of the sliding surface, a switched controller is designed so that the system state trajectories point towards the surface such that the state is driven to the this surface. Once system states reach to the sliding surface, they remain on it. This kind of controllers results in discontinuous closed-loop systems. [16]

The main concepts and notations of sliding mode control are presented first for systems with a single control input, which allow us to develop intuition about the basic aspects.

Let a single input nonlinear system be defined as

$$y^{(n)}(t) = f\left(\mathbf{x}(\mathrm{t}), t\right) + b\left(\mathbf{x}(\mathrm{t}), t\right)u(t) \tag{2.1}$$

Here, $\mathbf{x}(\mathrm{t})$ is the state vector, $u(t)$ is the control input and $y(t)$ is the output of interest.

The superscript (n) on $y(t)$ shows the order of differentiation and Eq. (2.1) implies that the explicit relationship between $y(t)$ and $u(t)$ can be established only after taking the n^{th} derivative of $y(t)$. $f(\mathbf{x}, t)$ and $b(\mathbf{x}, t)$ are generally nonlinear functions of $\mathbf{x}$ and t. The function $f(\mathbf{x}, t)$ is not exactly known, but the extent of the imprecision in $f(\mathbf{x}, t)$ is upper bounded by a known and continuous function of $\mathbf{x}$ and t. Similarly, the control gain $b(\mathbf{x}, t)$ is not exactly known, but it is of known sign and its uncertainty is bounded by known and continuous functions of $\mathbf{x}$ and t. The control problem is to get the state $\mathbf{x}$ to track a specific time-varying state $\mathbf{x}_{\mathrm{d}}$ in the presence of model imprecision in $f(\mathbf{x}, t)$ and $b(\mathbf{x}, t)$. A time varying surface $\Omega(t)$ is defined in the state space $\mathbf{R}^{(\mathbf{n})}$ by equating the variable $s(\mathbf{x}, t)$, defined below, to zero.

$$s(\mathbf{x}; t) = \left(\frac{d}{dt} + \delta\right)^{n-1} \tilde{y}(t) \tag{2.2}$$

Here, δ is a strictly positive constant, $\tilde{y}(t) = y(t) - y_d(t)$ and $\tilde{\mathbf{x}}(t) = \mathbf{x}(t) - \mathbf{x}_\mathrm{d}(t)$. The problem of tracking the *n*-dimensional vector $\mathbf{x}_\mathrm{d}(t)$ can in effect be replaced by a stabilisation problem in s.

The sliding surface Ω is defined by $s(\mathbf{x},t) = 0$ and the system's behaviour on the surface Ω is called sliding mode or sliding regime. From (2.2) it is seen that the expression of s contains $\tilde{y}^{(n-1)}$. So, by differentiating s only once, the input u to appears for the subsequent manipulations.

Furthermore, the bounds on s can be directly translated into bounds on the tracking error vector $\tilde{\mathbf{x}}$, and therefore the scalar s represents a true measure of the tracking performance. The corresponding transformations of performance measures assuming $\tilde{y}(0) = 0$ is:

$$\begin{aligned} &\forall t \geq 0,\ |s(t)| \leq \phi \ \Rightarrow\ \forall t \geq 0,\ \left|\tilde{y}^{(i)}(t)\right| \leq (2\delta)^i \varepsilon \\ &i = 0,.....,n-1 \end{aligned} \tag{2.3}$$

where $\varepsilon = \phi / \delta^{n-1}$. In this way, an n^{th} order tracking problem can be replaced by a 1st order stabilisation problem. The simplified, 1st order problem of keeping the scalar s at zero can now be achieved by choosing the control law u of (2.1) such that outside of $\Omega(t)$

$$\frac{1}{2}\frac{d}{dt}s^2 \leq -\eta|s| \tag{2.4}$$

where η is a strictly positive constant.

Condition (2.4) states that the squared "distance" to the surface, as measured by s^2, decreases along all the system trajectories.

Thus, it constrains trajectories to point towards the surface $\Omega(t)$. In particular, once on the surface, the system trajectories remain on the surface. In other words, satisfying the sliding condition makes the surface an invariant set (a set for which any trajectory starting from an initial condition within the set remains in the set for all times). Furthermore (2.4) also implies that some disturbances or dynamic uncertainties can be tolerated while still keeping the surface an invariant set.

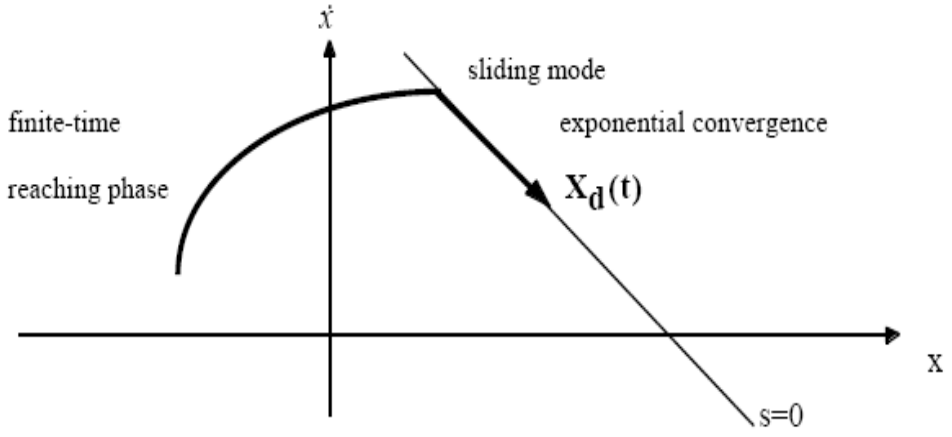

Figure 2.1 Graphical interpretation of equations (2.2) and (2.4) (n=2)
(Resource: Slotine and Li 1991, [11])

Finally, satisfying (2.4) guarantees that if condition $\mathbf{x}_{\mathrm{d}}(0)=\mathbf{x}(0)$ is not exactly verified, i.e., if $\mathbf{x}(t=0)$ is actually off $\mathbf{x}_{\mathrm{d}}(t=0)$, the surface $\Omega(t)$ will be reached in a finite time smaller than $|s(t=0)|/\eta$. Assume for instance that $s(t=0)>0$, and let t_{reach} be the time required to hit the surface $s=0$.

Integrating (2.4) between $t = 0$ and t_{reach} leads to

$$0-s(t=0)=s(t=t_{reach})-s(t=0) \;\leq\; -\eta\,(t_{reach}-0) \tag{2.5}$$

which implies that

$$t_{reach} \;\leq\; s(t=0)\,/\,\eta \tag{2.6}$$

The similar result starting with $s(t=0)<0$ can be obtained as

$$t_{reach} \;\leq\; |s(t=0)|\,/\,\eta \tag{2.7}$$

For initial condition, the state trajectory reaches the sliding surface in a finite time smaller than $|s(t=0)|\,/\,\eta$, and then slides on the surface towards $\mathbf{x}_{\mathrm{d}}(t)$ exponentially, with a time-constant equal to $1/\lambda$.

In summary, the idea is to use a well-behaved function of the tracking error, s, according to (2.2), and then select the feedback control law u in (2.1) such that s^2 remains a Lyapunov-like function of the closed-loop system, despite the presence of model imprecision and of disturbances.

2.1.2 Controller Design

The controller design procedure consists of two steps. First, one selects the feedback control law u as to verify sliding condition (2.4). However, the control law has to be discontinuous across $\Omega(t)$ in order to cope with the modelling imprecision and the disturbances. It is inapplicable to implement the associated control switching, since this result with chattering. Chattering is undesirable in practice, since it involves high control activity and may excite high frequency dynamics neglected in the course of modelling. Therefore, in the second step, an optimal trade-off between control bandwidth and tracking precision is accomplished by means of smoothing the discontinuous control law u in a suitable manner. [16]

As an example, consider a simple second order system described by

$$\ddot{x}(t) = f(x,t) + u(t) \tag{2.8}$$

where $f(x,t)$ is generally nonlinear and/or time/state varying and is estimated as $\hat{f}(x,t)$, $u(t)$ is the control input, and $x(t)$ is the state to be controlled so that it follows a desired trajectory $x_d(t)$. The estimation error in $f(x,t)$ is assumed to be bounded by some known function $F = F(x,t)$, so that

$$\left|\hat{f}(x,t) - f(x,t)\right| \leq F(x,t) \tag{2.9}$$

Let the distance to the sliding surface be defined according to (2.2). That is,

$$s(t) = \left(\frac{d}{dt} + \gamma \right) \tilde{x}(t) = \dot{\tilde{x}}(t) + \gamma \, \tilde{x}(t) \tag{2.10}$$

Differentiation of $s(t)$ yields

$$\dot{s}(t) = \ddot{x}(t) - \ddot{x}_d(t) + \gamma \, \dot{\tilde{x}}(t) \tag{2.11}$$

Substituting Equation (2.8) in Equation (2.11), $\dot{s}(t)$ becomes,

$$\dot{s}(t) = f\,(x,t) + u\left(t\right) - \ddot{x}_d(t) + \gamma \, \dot{\tilde{x}}(t) \tag{2.12}$$

The approximate control $\hat{u}\left(t\right)$ to achieve $\dot{s}(t) = 0$ is

$$\hat{u}\left(t\right) = \ddot{x}_d(t) - \gamma \, \dot{\tilde{x}}(t) - \hat{f}\,(x,t) \tag{2.13}$$

$\hat{u}\left(t\right)$ is the *nominal control* or the *sliding-phase control*, which would keep the system state on the sliding surface if $f\,(x,t)$ and $\hat{f}\,(x,t)$ were equal.

On the other hand, if $s(t) \neq 0$, i.e. if the system state is not on the sliding surface, it can be forced to be zero according to the following condition deduced from the Lyapunov's second stability theorem.

$$\frac{1}{2}\frac{d}{dt}(s^2(t)) = s(t)\dot{s}(t) \leq -\eta \left| s(t) \right| \tag{2.14}$$

This condition can be satisfied by the following control input,

$$u(t) = \hat{u}(t) - k(x,t)\ \mathrm{sgn}\left[s(t)\right] \tag{2.15}$$

With this control, Inequality (2.14) becomes

$$s(t)[f(x,t) + \hat{u}(t) - k(x,t)\mathrm{sgn}(s(t)) - \ddot{x}_d + \gamma\dot{\tilde{x}}(t)] \le -\eta\left|s(t)\right| \tag{2.16}$$

Let Eq. (2.13) be substituted. Then,

$$s(t)[f(x,t) - \hat{f}(x,t)] \le [k(x,t) - \eta]\left|s(t)\right| \tag{2.17}$$

In the worst case,

$$f(x,t) - \hat{f}(x,t) = F(x,t)\mathrm{sgn}[s(t)] \tag{2.18}$$

Then,

$$[k(x,t) - \eta - F(x,t)]\left|s(t)\right| \ge 0 \tag{2.19}$$

Hence, by choosing $k(x,t)$ large enough, such as

$$k\left(x,t\right) > F\left(x,t\right) + \eta \tag{2.20}$$

the satisfaction of condition (2.14) can be ensured.

The preceding simple example shows the main advantages of transforming the original tracking problem into a simple 1st order stabilisation problem for the variable *s*.

In the first-order systems, the intuitive feedback control strategy "if the error is negative, push on to the positive direction; if the error is positive, push on to the negative direction" works. The same statement is not true in a general higher-order system.

Now consider the second order system described by,

$$\ddot{x}(t) = f(x,t) + b(x,t)\,u(t) \tag{2.21}$$

where $b(x,t)$ is bounded as

$$0 < b_{min}(x,t) < b(x,t) < b_{max}(x,t) \tag{2.22}$$

The control gain $b(x,t)$ and its bound can be time varying or state dependent. Since the control input enters multiplicatively in the dynamics, the geometric mean of the lower and upper bound of the gain is a reasonable estimate:

$$\hat{b}(x,t) = \sqrt{b_{min}(x,t)\; b_{max}(x,t)} \tag{2.23}$$

Bounds can then be written in the form

$$\beta^{-1} \le \frac{\hat{b}}{b} \le \beta \tag{2.24}$$

where $\beta = \left(b_{\max} / b_{\min}\right)^{1/2}$

Since the control law will be designed to be robust to the bounded multiplicative uncertainty, β is called the margin of the design.

It can be proved that the control law

$$u(t) = \hat{b}(\mathrm{x,t})^{-1}[\hat{u}(t) - k(x,t)\ \mathrm{sgn}\{s(t)\}] \tag{2.25}$$

with

$$k(x,t) \geq \beta(x,t)(F(x,t) + \eta) + [\beta(x,t) - 1]|\hat{u}(t)| \tag{2.26}$$

satisfies the condition (2.14), or sliding condition.

The control law for a higher order system can be derived based on a similar approach.

2.1.3 Summary

By courtesy of its robustness properties, sliding mode controller provides good performance for the following two cases which can be defined as two major design difficulties encountered in the design of a control algorithm:

1. The system is nonlinear with time-varying parameters and uncertainties;
2. The performance of the system depends strongly on the knowledge of the disturbances;

For the class of systems to which it applies, sliding mode controller design provides a systematic approach to the problem of maintaining stability and consistent performance in the face of modelling imprecision. The main advantage of sliding mode control is that the system's response remains insensitive to some kinds of model uncertainties and disturbances.

A generic hypersonic air vehicle model is used in this thesis as a case study example to observe the performance of the proposed sliding mode controller. The problem can be summarised as to design a nonlinear and time-varying control system for tracking velocity and altitude commands under the presence of disturbance for this hypersonic air vehicle. Hypersonic air vehicles are sensitive to changes in flight condition as well as physical and aerodynamic parameters due to their design and flight conditions of high altitudes and Mach numbers. For example, at cruise flight at an altitude of 110,000 ft and Mach 15, a 1-deg increase in the angle of attack produces a relatively large load factor. Furthermore, it is difficult to measure or estimate the atmospheric properties and aerodynamic characteristics at high flight altitudes.

As a result; modelling inaccuracies can result and can have strong adverse effects on the performance of the air vehicle's control systems. Therefore, employing a kind of robust control has been the main technique used for hypersonic flight control. [10]

The sliding mode control, which is one of the most important robust control techniques, provides a systematic approach to the problem of maintaining stability and consistent performance in the face of modelling imprecision. The main advantage of sliding mode control is that the system's response remains insensitive to model uncertainties and disturbances. On the other hand, the sliding mode control requires a trade-off between robustness properties against model uncertainties and disturbances and control system performances. It is meant that the sliding mode control has drawbacks like large control effort necessity and chattering in the face of model uncertainties and disturbances. The performance of the sliding mode controller can be increased and these drawbacks can be eliminated by combining the sliding mode controller with an adaptive scheme. [10]

2.2 SMC Design Methodology Used in This Study

SMC design for nonlinear systems has been studied by various researchers [3, 7, 11, 18, 23]. It is well-known that there is no straight forward method to design sliding surface for nonlinear systems since ensuring the stability of sliding motion requires special assessment for the nonlinear system under consideration. Therefore, sliding surface design for nonlinear systems is still an active research field in SMC theory.

In this thesis, a relatively systematic method is proposed to design sliding surface for nonlinear systems given by the following expression.

$$\dot{\mathbf{x}} = \mathbf{A}(\mathbf{x})\mathbf{x} + \mathbf{B}(\mathbf{x})\mathbf{u} \tag{2.27}$$

where $\mathbf{x} \in \Re^n$ and $\mathbf{u} \in \Re^m$ are the state and control vectors and $\mathbf{A}(\mathbf{x}) \in \Re^{n\times n}$ and $\mathbf{B}(\mathbf{x}) \in \Re^{n\times m}$ are nonlinear State Dependent Coefficient (SDC) matrices. Equation (2.27) is a special representation of the nonlinear dynamics described by the following equation,

$$\dot{\mathbf{x}} = \mathbf{a}(\mathbf{x}) + \mathbf{B}(\mathbf{x})\mathbf{u} \tag{2.28}$$

where $\mathbf{a}(\mathbf{x}) = \mathbf{A}(\mathbf{x})\mathbf{x}$ and $\mathbf{A}(\mathbf{x})$ is obtained by using the so-called SDC parameterisation [15].

The nonlinear dynamics given by (2.27) is studied by various authors in order to design optimal controllers.

One of the recent approaches to the optimal controller design for the nonlinear system is the so-called State Dependent Riccati Equations (SDRE) method [15, 28, 38, 39]. The basic idea in SDRE is to extend classical Linear Quadratic Regulator (LQR) method to the nonlinear system equations. As seen in (2.27), the nonlinear system equation is an extension of $\dot{\mathbf{x}} = \mathbf{A}\mathbf{x} + \mathbf{B}\mathbf{u}$ type Linear Time Invariant (LTI) system which is well studied in terms of both optimal and state-feedback controls in the literature. Therefore by extending the control theory for LTI systems to (2.27), it may be possible to design similar type of controllers for the nonlinear system.

One of the problems of SDRE based control design for nonlinear systems is to ensure the system stability. Unfortunately, there are no global stability results seen in the literature. Nevertheless, local asymptotical stability of SDRE based optimal control for the nonlinear system given by (2.27) is proved by different authors. For the sake of completeness, the local stability result of [15] is given below without its proof.

Theorem 1

Assume that the SDC parameterisation is chosen such that $\mathrm{col}\{\mathbf{A}(\mathbf{x})\} \in \square^1$ in the neighbourhood Ω about the origin that the pair $\{\mathbf{A}(\mathbf{x}), \mathbf{B}(\mathbf{x})\}$ is pointwise stabilisable in the linear sense for all $\mathbf{x} \in \Omega$. Then the SDRE nonlinear regulator produces a closed-loop solution which is locally asymptotically stable [15].

Another problem in the SDRE based controller design is to accomplish the SDC parameterisation since the parameterisation is not unique. However, one of the most important factors in the parameterisation process is to assure the pointwise controllability in the local region.

The details of SDRE theory and simulation results together with some real applications can be found in [15, 28, 38, 39].

As can be seen in equation (2.27), there is no uncertain dynamics or disturbance effects in the nonlinear expressions. Although it is possible to use the idea of SDRE in order to design SMC for (2.27), the disturbance (or modelling uncertainty) term is included into the nonlinear dynamics to emphasise the disturbance rejection capability of the SMC. With this approach, SMC is combined with SDRE which enables one to design SMC for a class of nonlinear systems in a relatively systematic manner. Besides, by using State Dependent parameters in sliding surface definition, the SMC can adapt the controller against the nonlinearities and disturbances of the system which may be regarded as an Adaptive Sliding Mode Control (ASMC). The method is given in the following section.

2.2.1 SMC Combined with SDRE (Adaptive Sliding Mode Control)

The system to be controlled with this methodology is described as follows.

$$\dot{\mathbf{x}} = \mathbf{A}(\mathbf{x})\mathbf{x} + \mathbf{B}(\mathbf{x})\mathbf{u} + \mathbf{f}(\mathbf{x}) + \mathbf{d}(\mathbf{x}) \tag{2.29}$$

where $\mathbf{x} \in \Re^n$ and $\mathbf{u} \in \Re^m$ are the state and control vectors. Here, $\mathbf{f(x)} \in \Re^n$ is a nonlinear vector which includes the terms remained after SDC parameterisation and/or the constant terms of the state dependent disturbance vector. As for **d(x)**, it is the state-dependent disturbance vector.

SDRE control design method is based on freezing the nonlinear dynamics at the given operating point and designing the controller at that operating point. In other words, pointwise controller design is accomplished and control parameters are updated at each operating point. Therefore, linear control design techniques (which are updated at each operating point) can be used for the nonlinear system.

SMC design for LTI systems are studied thoroughly in the literature (see [2] and [4] for more details). In this study, the SMC design method for LTI systems is used and is extended to the nonlinear dynamics. As in the case of SDRE based controller design, the nonlinear system is frozen at each operating point and pointwise SMC is designed for each LTI dynamics. In order to design SMC for the LTI system, the system is transformed so that it can be separated into two parts such that one of the parts is in the so-called reduced order form in which the control inputs are absent. The transformed system is to be represented by an equation such as,

$$\dot{\mathbf{z}} = \mathbf{A}_z\mathbf{z} + \mathbf{B}_z\mathbf{u} + \mathbf{f}_z + \mathbf{d}_z \tag{2.30}$$

where

$$\mathbf{A}_z = \left[\begin{array}{c|c} \mathbf{A}_{z11} & \mathbf{A}_{z12} \\ \hline \mathbf{A}_{z21} & \mathbf{A}_{z22} \end{array}\right],\ \mathbf{B}_z = \left[\begin{array}{c|c} \mathbf{0} & \mathbf{0} \\ \hline \mathbf{B}_{21} & \mathbf{B}_{21} \end{array}\right],\ \mathbf{F}_z = \left[\begin{array}{c} \mathbf{f}_{1z} \\ \hline \mathbf{f}_{2z} \end{array}\right],\ \mathbf{D}_z = \left[\begin{array}{c} \mathbf{d}_{1z} \\ \hline \mathbf{d}_{2z} \end{array}\right] \tag{2.31}$$

and $\mathbf{B}_2 = \left[\mathbf{B}_{21} \,\vdots\, \mathbf{B}_{22}\right]$ is non-singular. In the expanded form, the equation becomes,

$$\left[\begin{array}{c} \dot{\mathbf{z}}_1 \\ \hline \dot{\mathbf{z}}_2 \end{array}\right] = \left[\begin{array}{c|c} \mathbf{A}_{z11} & \mathbf{A}_{z12} \\ \hline \mathbf{A}_{z21} & \mathbf{A}_{z22} \end{array}\right]\left[\begin{array}{c} \mathbf{z}_1 \\ \hline \mathbf{z}_2 \end{array}\right] + \left[\begin{array}{c|c} \mathbf{0} & \mathbf{0} \\ \hline \mathbf{B}_{21} & \mathbf{B}_{21} \end{array}\right]\left[\begin{array}{c} \mathbf{u}_1 \\ \hline \mathbf{u}_2 \end{array}\right] + \left[\begin{array}{c} \mathbf{f}_{1z} \\ \hline \mathbf{f}_{2z} \end{array}\right] + \left[\begin{array}{c} \mathbf{d}_{1z} \\ \hline \mathbf{d}_{2z} \end{array}\right] \tag{2.32}$$

The required transformation described above can be achieved by the following equation

$$\mathbf{z} = \mathbf{T}\mathbf{x} \tag{2.33}$$

where $\mathbf{z}$ is the new state vector and $\mathbf{T}$ is the state transformation matrix which is assumed to be non-singular.

The state transformation matrix $\mathbf{T}$ is not unique and there are different methods to obtain it. One of the methods to find the transformation matrix is the use of "QR decomposition" technique.

The QR decomposition (also called the QR factorisation) of a matrix is a decomposition of the matrix into an orthonormal (or unitary) matrix **Q** and a right triangular matrix **R** as indicated below.

$$\mathbf{A} = \mathbf{QR} \tag{2.34}$$

There are several methods for finding the QR decomposition, such as by means of the Gram–Schmidt process, Householder transformations, or Givens rotations. Each has a number of advantages and disadvantages. In this study, the special command of MATLAB, "qr" is used. It is used as described below.

[**Tr** : **Temp**] = qr(**B**)

Here **Temp** stands for a temporarily constructed matrix while **Tr** stands for the matrix constructed for the transformation. This produces an upper triangular matrix **Temp** of the same dimension as **B** and a unitary matrix **Tr** so that $\mathbf{B} = \mathbf{Tr} \times \mathbf{Temp}$. For sparse matrices, **Tr** is often nearly full. If **B** is an $m \times n$ matrix, then **Tr** is $m \times m$ and **Temp** is $m \times n$.

In the next step, **Tr** matrix is inverted first and its rows are re-ordered to reach the final state transformation matrix **T** such that

$$\mathbf{B}_z = \mathbf{TB} \tag{2.35}$$

As a case study, consider the nonlinear dynamics of a hypersonic air vehicle model which is used in Chapter 3. The state and control vectors are,

$$\mathbf{x} = \begin{bmatrix} \tilde{x}_1 \\ x_2 \\ \tilde{x}_3 \\ x_4 \\ x_5 \end{bmatrix} = \begin{bmatrix} \tilde{V} \\ \gamma \\ \tilde{h} \\ \alpha \\ q \end{bmatrix} \text{ and,} \tag{2.36}$$

$$\mathbf{u} = \begin{bmatrix} u_1 \\ u_2 \end{bmatrix} = \begin{bmatrix} \delta_e \\ \beta \end{bmatrix} \tag{2.37}$$

Here, the state variables are the percentage change in the velocity relative to its initial value, the flight path angle, the percentage change in the altitude relative to its initial value, the angle of attack and the pitch rate. On the other hand, the control inputs, u_1 and u_2 are the elevator deflection and the throttle setting.

As the first and third system state variables, the percentage changes of the velocity and altitude are used to make all the state variables have comparable orders of magnitudes. Otherwise, the difference between the orders of magnitude of the first and third system state variables and the remaining ones happens to be very large and this leads to some difficulties in numerical computing. These percentage changes are defined as follows;

$$\tilde{V} = \frac{V - V_0}{V_0} \Rightarrow \tilde{x}_1 = \frac{x_1 - x_{10}}{x_{10}} \tag{2.38}$$

therefore,

$$x_1 = x_{10}\left(1 + \tilde{x}_1\right) \tag{2.39}$$

and,

$$\dot{x}_1 = \dot{\tilde{x}}_1 x_{10} \tag{2.40}$$

$$\tilde{h} = \frac{h - h_0}{h_0} \Rightarrow \tilde{x}_3 = \frac{x_3 - x_{30}}{x_{30}} \tag{2.41}$$

therefore,

$$x_3 = x_{30}\left(1 + \tilde{x}_3\right) \tag{2.42}$$

and,

$$\dot{x}_3 = \dot{\tilde{x}}_3 x_{30} \tag{2.43}$$

where V_0 and x_{10} are the initial values of the velocity and h_0 and x_{30} are the initial values of the altitude.

The term $\mathbf{f}(\mathbf{x})$ in (2.29) gets added to the system differential equation as a result of the new definition of the first and third system state variables in the form of percentages. This term is taken into account as a known disturbance and it is compensated by the designed controller.

The derivation of the state transformation matrix is shown below for the **B** matrix used in the simulations of this study.

$$\mathbf{B} = \begin{bmatrix} 0 & b_{12} \\ 0 & b_{22} \\ 0 & 0 \\ 0 & b_{42} \\ b_{51} & b_{52} \end{bmatrix} = \left[\mathbf{Tr}\right]_{5x5} \mathrm{x} \left[\mathbf{Temp}\right]_{5x2} \tag{2.44}$$

$$\mathbf{Temp} = \begin{bmatrix} a & 0 \\ 0 & b \\ 0 & 0 \\ 0 & 0 \\ 0 & 0 \end{bmatrix} \tag{2.45}$$

where *a* and *b* are the values obtained by the QR decomposition.

Note that,

$$\mathbf{Temp} = \begin{bmatrix} a & 0 \\ 0 & b \\ 0 & 0 \\ 0 & 0 \\ 0 & 0 \end{bmatrix} = \mathbf{Tr}^{-1}\mathbf{B} \tag{2.46}$$

By simply re-ordering the elements of $\mathbf{Tr}^{-1}$, the final state transformation matrix $\mathbf{T}$ can be obtained such that the desired form is achieved as shown below,

$$\mathbf{TB} = \begin{bmatrix} 0 & 0 \\ 0 & 0 \\ 0 & 0 \\ a & 0 \\ 0 & b \end{bmatrix} = \mathbf{TB} = \mathbf{B}_z \tag{2.47}$$

In other words, this state transformation matrix is used to obtain the reduced order forms of the system matrices $\mathbf{A}_z$, $\mathbf{B}_z$, $\mathbf{F}_z$ and $\mathbf{D}_z$. The derivation of these matrices is explained in the following part. By assuming a time varying and/or a state dependent state transformation such as

$$\mathbf{z} = \mathbf{Tx} \tag{2.48}$$

and its derivative,

$$\dot{\mathbf{z}} = \mathbf{T}\dot{\mathbf{x}} + \dot{\mathbf{T}}\mathbf{x} = \mathbf{TAx} + \mathbf{TBu} + \dot{\mathbf{T}}\mathbf{x} = (\mathbf{TA} + \dot{\mathbf{T}})\mathbf{x} + \mathbf{TBu} + \mathbf{Tf} + \mathbf{Td} \tag{2.49}$$

the new state equation is obtained as,

$$\dot{\mathbf{z}} = \mathbf{A}_z\mathbf{z} + \mathbf{B}_z\mathbf{u} + \mathbf{f}_z + \mathbf{d}_z \tag{2.50}$$

Dimensions of the vector and matrix variables are given here to prevent any misunderstanding.

$\mathbf{x} \in \Re^n$	$\mathbf{z} \in \Re^n$	$\mathbf{B}_2 \in \Re^{m \times m}$	$\mathbf{A}_{z21} \in \Re^{mx(n-m)}$	$\mathbf{f}_{2z} \in \Re^m$
$\mathbf{u} \in \Re^m$	$\mathbf{z}_1 \in \Re^{n-m}$	$\mathbf{A}_{z11} \in \Re^{(n-m)\times(n-m)}$	$\mathbf{A}_{z22} \in \Re^{mxm}$	$\mathbf{d}_{1z} \in \Re^{(n-m)}$
$\mathbf{B} \in \Re^{nxm}$	$\mathbf{z}_2 \in \Re^m$	$\mathbf{A}_{z12} \in \Re^{(n-m)\times m}$	$\mathbf{f}_{1z} \in \Re^{(n-m)}$	$\mathbf{d}_{2z} \in \Re^m$

Here *n* is the number of state variables and *m* is the number of control inputs.

As a useful reminder, $\mathbf{d_{1z}}$ is the disturbance input to the reduced order system (i.e. the first subsystem without the control inputs) while $\mathbf{d_{2z}}$ is the disturbance input to the second subsystem with the control inputs. Similarly, $\mathbf{f_{1z}}$ is the additional known input to the reduced order system and $\mathbf{f_{2z}}$ is the additional known input to the second subsystem. It is to be noted that, $\mathbf{d_{1z}}$ is not taken into account in the controller design because there is no control input in the first part of the system. It is expected that this disturbance input is compensated by the disturbance rejection capability of the sliding mode controller.

The first part of the new state equations is

$$\dot{\mathbf{z}}_1 = \mathbf{A}_{z11}\mathbf{z}_1 + \mathbf{A}_{z12}\mathbf{z}_2 + \mathbf{f_{1z}} + \mathbf{d_{1z}} \tag{2.51}$$

The above part is called as the "indirectly controlled subsystem" since there is no control term.

On the other hand, all the control effort is lumped into the second part, which is called as the "directly controlled subsystem". The state equation of this subsystem is,

$$\dot{\mathbf{z}}_2 = \mathbf{A}_{z21}\mathbf{z}_1 + \mathbf{A}_{z22}\mathbf{z}_2 + \mathbf{B}_2\mathbf{u} + \mathbf{f_{2z}} + \mathbf{d_{2z}} \tag{2.52}$$

The control effort is transmitted to the indirectly controlled first subsystem through the state vector $\mathbf{z}_2$ of the directly controlled subsystem.

This transmission is realised by treating $\mathbf{z}_2$ as if it is the control input to the first subsystem. As such, it is formulated most typically according to the state variable feedback control law so that

$$\mathbf{z}_2 = \mathbf{h}_2 - \mathbf{C}\mathbf{z}_1 \tag{2.53}$$

Here, $\mathbf{h}_2$ is the bias term added for the purpose of disturbance rejection and $\mathbf{C}$ is the feedback gain matrix. Note that Eq. (2.53) defines a surface Ω (i.e. a $n-m$ dimensional manifold) in the n dimensional state space of the whole system. This surface is called the sliding surface. The deviation $\boldsymbol{\sigma}$ of the state vector from the sliding surface is expressed as,

$$\boldsymbol{\sigma}(\mathbf{z}) = \mathbf{z}_2 + \mathbf{C}\mathbf{z}_1 - \mathbf{h}_2 \tag{2.54}$$

Using the surface-related terminology, $\mathbf{C}$ is considered as the slope of the sliding surface and $\mathbf{h}_2$ is considered as the offset of the sliding surface from the origin of the state space. $\mathbf{h}_2$ term is deliberately added to the classical sliding surface equation in order to suppress the effects of $\mathbf{f}_{1z}$ and $\mathbf{d}_{1z}$ in (2.51) as much as possible.

When the system state is on the sliding surface, i.e. when $\boldsymbol{\sigma}(\mathbf{z}) = \mathbf{z}_2 + \mathbf{C}\mathbf{z}_1 - \mathbf{h}_2 = 0$, Eq. (2.51) becomes;

$$\dot{\mathbf{z}}_1 = (\mathbf{A}_{z11} - \mathbf{A}_{z12}\mathbf{C})\mathbf{z}_1 + (\mathbf{A}_{z12}\mathbf{h}_2 + \mathbf{f}_{1z} + \mathbf{d}_{1z}) \tag{2.55}$$

Here, $\mathbf{C}$ and $\mathbf{h_2}$ must be determined in such a way that the closed-loop system represented by Eq. (2.55) is asymptotically stable with a sufficiently fast convergence and $\mathbf{z}_1$ approaches the desired vector $\mathbf{z}_{1d}$ with a tolerable error.

After the sliding surface is determined as described above, the next stage of controller design is to determine the actual control vector **u** so that the state of the system is forced toward the sliding surface. In other words, **u** must be determined so that $\boldsymbol{\sigma}$ is driven to zero and kept so despite the disturbances. This purpose can be achieved by using the second stability theorem of Lyapunov as described below.

Let $\mathbf{V} = \frac{1}{2}\boldsymbol{\sigma}^{\mathrm{T}}\boldsymbol{\sigma}$ be defined as the Lyapunov function. Then, the following condition must be satisfied to force $\boldsymbol{\sigma}$ to be zero.

$$\dot{\mathbf{V}} = \boldsymbol{\sigma}^{\mathrm{T}}\dot{\boldsymbol{\sigma}} < 0 \tag{2.56}$$

This condition leads to the sliding mode controller (SMC) through the following stages.

Recalling $\boldsymbol{\sigma}(\mathbf{z})$ from equation (2.54), its derivative is written as

$$\dot{\boldsymbol{\sigma}}(\mathbf{z}) = \dot{\mathbf{z}}_2 + \mathbf{C}\dot{\mathbf{z}}_1 + \dot{\mathbf{C}}\mathbf{z}_1 - \dot{\mathbf{h}}_2 \tag{2.57}$$

$$\dot{\boldsymbol{\sigma}}(\mathbf{z}) = \mathbf{A}_{z21}\mathbf{z}_1 + \mathbf{A}_{z22}\mathbf{z}_2 + \mathbf{B}_2\mathbf{u} + \mathbf{f}_{2z} + \mathbf{d}_{2z} + \mathbf{C}(\mathbf{A}_{z11}\mathbf{z}_1 + \mathbf{A}_{z12}\mathbf{z}_2 + \mathbf{f}_{1z} + \mathbf{d}_{1z}) + \dot{\mathbf{C}}\mathbf{z}_1 - \dot{\mathbf{h}}_2 \tag{2.58}$$

By using the condition that $\boldsymbol{\sigma}^{\mathrm{T}}\dot{\boldsymbol{\sigma}} < 0$; SMC can be obtained as follows being composed of two different controllers, i.e. as $\mathbf{u} = \mathbf{u}_{\mathrm{nom}} + \mathbf{u}_{\mathrm{sw}}$.

(i) The nominal control:

$$\mathbf{u}_{\mathrm{nom}} = -\mathbf{B}_2^{-1}\left[\mathbf{A}_{z21}\mathbf{z}_1 + \mathbf{A}_{z22}\mathbf{z}_2 + \mathbf{f}_{2\mathbf{z}} + \mathbf{C}(\mathbf{A}_{z11}\mathbf{z}_1 + \mathbf{A}_{z12}\mathbf{z}_2 + \mathbf{f}_{1\mathbf{z}}) + \dot{\mathbf{C}}\mathbf{z}_1 - \dot{\mathbf{h}}_{\mathbf{2}}\right] \quad (2.59)$$

As noticed, the disturbances $\mathbf{d}_{1\mathbf{z}}$ and $\mathbf{d}_{2\mathbf{z}}$ are assumed to be zero in obtaining the nominal control.

(ii) The switching control:

$$\mathbf{u}_{\mathrm{sw}} = -\mathbf{B}_2^{-1}\mathbf{K}\begin{bmatrix}\mathrm{sgn}(\sigma_1)\\ \mathrm{sgn}(\sigma_2)\end{bmatrix} \quad (2.60)$$

This control constituent is added in order to deal with the disturbances $\mathbf{d}_{1\mathbf{z}}$ and $\mathbf{d}_{2\mathbf{z}}$. Its derivation is explained below.

When equation (2.59) is substituted, Inequality (2.56) becomes,

$$\boldsymbol{\sigma}^{\mathrm{T}}\dot{\boldsymbol{\sigma}} = \boldsymbol{\sigma}^{\mathrm{T}}\left[\mathbf{B}_2\mathbf{u}_{\mathrm{sw}} + \mathbf{d}_{2\mathbf{z}} + \mathbf{C}\mathbf{d}_{1\mathbf{z}}\right] < 0 \quad (2.61)$$

or,

$$\boldsymbol{\sigma}^{\mathrm{T}}\mathbf{B}_2\mathbf{u}_{\mathrm{sw}} + \boldsymbol{\sigma}^{\mathrm{T}}\left[\mathbf{d}_{2\mathbf{z}} + \mathbf{C}\mathbf{d}_{1\mathbf{z}}\right] < 0 \quad (2.62)$$

Let,

$$\mathbf{d}_{\text{eq}} = \mathbf{d}_{2\mathbf{z}} + \mathbf{C}\mathbf{d}_{1\mathbf{z}} \quad \text{and} \quad \mathbf{u}_{\text{sw}}{}' = \mathbf{B}_2\mathbf{u}_{\text{sw}} \tag{2.63}$$

Then,

$$\boldsymbol{\sigma}^{\text{T}}\mathbf{u}_{\text{sw}}{}' + \boldsymbol{\sigma}^{\text{T}}\mathbf{d}_{\text{eq}} < 0 \tag{2.64}$$

or,

$$\sigma_1 u_{\text{sw1}}{}' + \sigma_2 u_{\text{sw2}}{}' + \sigma_1 d_{\text{eq1}} + \sigma_2 d_{\text{eq2}} < 0 \tag{2.65}$$

Assume that,

$$\left|d_{\text{eq1}}\right| < D_1 \text{ and } \left|d_{\text{eq2}}\right| < D_2 \tag{2.66}$$

In the worst case,

$$d_{\text{eq1}} = D_1 \,\text{sgn}(\sigma_1) \text{ and } d_{\text{eq2}} = D_2 \,\text{sgn}(\sigma_2) \tag{2.67}$$

Then,

$$\sigma_1 u_{\text{sw1}}{}' + \sigma_2 u_{\text{sw2}}{}' + D_1\left|\sigma_1\right| + D_2\left|\sigma_2\right| < 0 \tag{2.68}$$

This condition can be satisfied by letting,

$$u_{\text{sw1}}{}' = -k_1 D_1 \,\text{sgn}(\sigma_1) \tag{2.69}$$

and

$$u_{sw2}' = -k_2 D_2 \operatorname{sgn}(\sigma_2) \tag{2.70}$$

Such that,

$$k_1 > 1 \text{ and } k_2 > 1 \tag{2.71}$$

Hence, $\mathbf{u}_{sw}$ can be obtained as,

$$\mathbf{u}_{sw} = \mathbf{B}_2^{-1}\mathbf{u}_{sw}' = -\mathbf{B}_2^{-1}\mathbf{K}\begin{bmatrix} \operatorname{sgn}(\sigma_1) \\ \operatorname{sgn}(\sigma_2) \end{bmatrix} \tag{2.72}$$

where,

$$\mathbf{K} = \begin{bmatrix} k_1 D_1 & 0 \\ 0 & k_2 D_2 \end{bmatrix} \tag{2.73}$$

As a summary, SMC can be obtained as the sum of the following two control constituents.

$$\mathbf{u}_{nom} = -\mathbf{B}_2^{-1}\left[\mathbf{A}_{z21}\mathbf{z}_1 + \mathbf{A}_{z22}\mathbf{z}_2 + \mathbf{f}_{2\mathbf{z}} + \mathbf{C}(\mathbf{A}_{z11}\mathbf{z}_1 + \mathbf{A}_{z12}\mathbf{z}_2 + \mathbf{f}_{1\mathbf{z}}) + \dot{\mathbf{C}}\mathbf{z}_1 - \dot{\mathbf{h}}_{\mathbf{2}}\right] \tag{2.74}$$

$$\mathbf{u}_{sw} = -\mathbf{B}_2^{-1}\mathbf{K}\begin{bmatrix} \operatorname{sgn}(\sigma_1) \\ \operatorname{sgn}(\sigma_2) \end{bmatrix} \tag{2.75}$$

In other words,

$$\mathbf{u} = \mathbf{u}_{nom} + \mathbf{u}_{sw} \tag{2.76}$$

Here $\mathbf{K}$ is a matrix of tuning parameters for adjusting how fast the system state will reach the sliding surface and how successfully the controller rejects the disturbances. In other words, $\mathbf{K}$ has two functions: disturbance rejection function and forcing function on the state to drive it toward the sliding surface. Its first function is explained above during the derivation. Its second function can be explained as follows.

- If $\mathbf{K}$ has small elements, reaching to the sliding surface is slow, but the chattering amplitude and frequency are also small.

- If $\mathbf{K}$ has large elements, reaching to the sliding surface is fast, but the chattering amplitude and frequency are also large.

Here, chattering is defined as the in-and-out oscillation of the system state about the sliding surface. This phenomenon arises due to the conflict between the distracting effect of the disturbances and the restoring effect of the switching parts of the control inputs.

As a summary, the larger the elements of $\mathbf{K}$ are, the more effective its two functions become, but on the other hand, the more severely the chattering phenomenon occurs. Figure 2.2 shows the effect of $\mathbf{K}$ on the chattering phenomenon. The “k” value in the figure is the amplitude of the chattering and it is directly proportional to the elements of the selected $\mathbf{K}$.

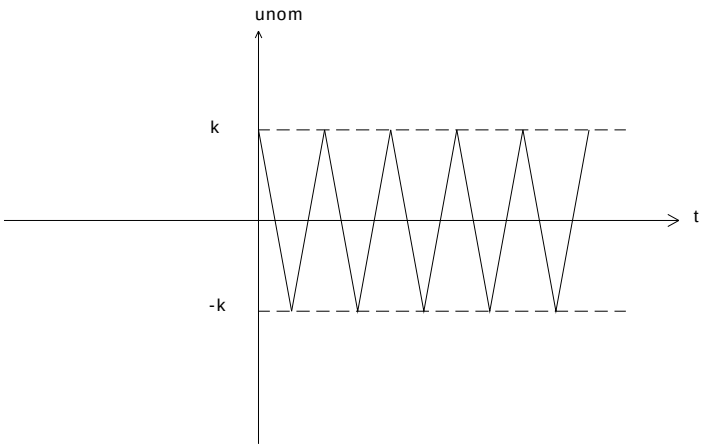

Figure 2.2 Effect of **K** on the Chattering Phenomenon

Figure 2.3 is given to explain the characteristic behaviour of the sliding mode controller which is composed of two sub-controllers. The first part is defined as the reaching phase and this is the part where the switching control is active and forces the system states towards the sliding surface. The second part is defined as the sliding phase and this is the part where the nominal control is active and keeps the system states on the sliding surface.

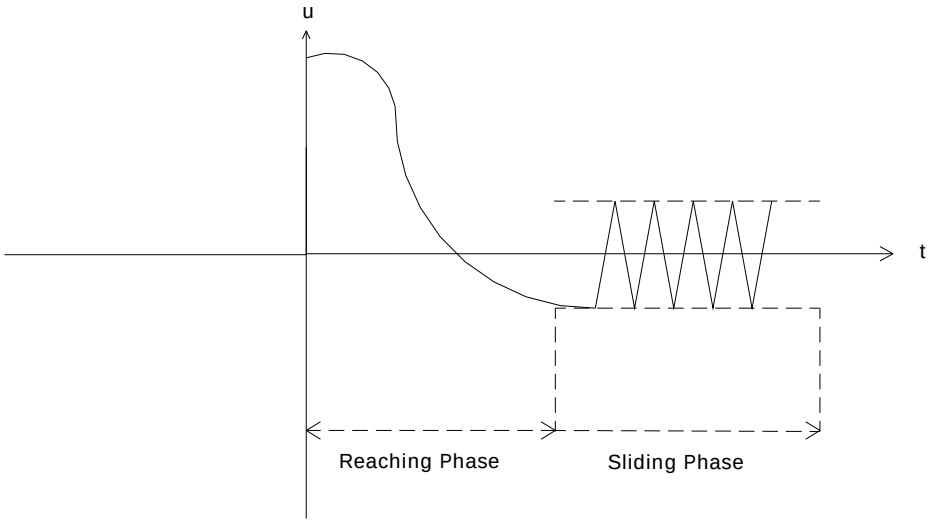

Figure 2.3 Typical SMC Input

2.2.1.1 Determination of Sliding Surface Parameters

At first, sliding surface equation is defined, $\boldsymbol{\sigma}(\mathbf{z}) = \mathbf{z}_2 + \mathbf{C}\mathbf{z}_1 - \mathbf{h}_2$, and then the sliding mode controller is designed based on this definition. But the parameters of the sliding surface equation: sliding surface slope matrix, $\mathbf{C}$ and the offset of sliding surface from the state space origin, $\mathbf{h}_2$ are still not known.

There are different methods for determining the slope and the offset of the sliding surface but in this study, they are determined by solving the State Dependent Riccati Equations (SDRE) so that they become adaptive to the nonlinearities of the system. By this methodology, the problem of sliding surface determination is reduced to a Linear Quadratic Regulator (LQR) problem including bias terms.

In other words, the slope ($\mathbf{C}$) and the offset ($\mathbf{h_2}$) of the sliding surface are determined so as to minimise the following cost functional.

$$J = \frac{1}{2}\int_{t_s}^{\infty}\left(\left(\mathbf{z}_1 - \mathbf{r}_1\right)^{\mathrm{T}}\mathbf{Q}_{11}\left(\mathbf{z}_1 - \mathbf{r}_1\right) + \left(\mathbf{z}_2 - \mathbf{r}_2\right)^{\mathrm{T}}\mathbf{Q}_{22}\left(\mathbf{z}_2 - \mathbf{r}_2\right)\right)\mathrm{dt} \tag{2.77}$$

Here, $\mathbf{r}_1$ represents the steady state values at the desired position for the reduced order system while $\mathbf{r}_2$ represents the steady state values at the desired position for the second subsystem. $\mathbf{Q}_{11}$ and $\mathbf{Q}_{22}$ are properly specified weighting matrices which may be functions of the state variables if desired. The desired final values of the state variables are expressed in more detail as follows.

$$\begin{bmatrix} \mathbf{r}_1 \\ \mathbf{r}_2 \end{bmatrix} = \mathbf{T}\mathbf{x}_\mathbf{d} = \mathbf{T}\begin{bmatrix} x_{d1} \\ x_{d2} \\ x_{d3} \\ x_{d4} \\ x_{d5} \end{bmatrix} = \begin{bmatrix} r_{11} \\ r_{12} \\ r_{13} \\ r_{21} \\ r_{22} \end{bmatrix} \Rightarrow \tag{2.78}$$

$$\mathbf{r}_1 = \begin{bmatrix} r_{11} \\ r_{12} \\ r_{13} \end{bmatrix} \quad \text{and,} \tag{2.79}$$

$$\mathbf{r}_2 = \begin{bmatrix} r_{21} \\ r_{22} \end{bmatrix} \tag{2.79}$$

where $\mathbf{x}_\mathbf{d}$ includes the steady state values for the system state variables.

In the general multivariable case, the SDRE nonlinear feedback solution and its associated state and costate trajectories satisfy the first necessary condition for optimality ($\partial \mathbf{H} / \partial \mathbf{z}_2 = 0$) of the nonlinear optimal regulator problem (2.77). Additionally, if $\mathbf{A}_{z11}$, $\mathbf{A}_{z12}$, $\mathbf{Q}_{11}$ and $\mathbf{Q}_{22}$ along with their gradients are bounded in a neighborhood about the origin, under asymptotic stability, as the state $\mathbf{z}_1$ is driven to zero, the second ecessary condition for optimality ($\dot{\boldsymbol{\lambda}}_1 = -\partial \mathbf{H} / \partial \mathbf{z}_1$) asymptotically satisfied at a quadratic rate. [28]

where **H** represents the Hamiltonian function and defined by,

$$\mathbf{H} = \frac{1}{2}\left(\mathbf{z}_1 - \mathbf{r}_1\right)^{\mathrm{T}} \mathbf{Q}_{11}\left(\mathbf{z}_1 - \mathbf{r}_1\right) + \frac{1}{2}\left(\mathbf{z}_2 - \mathbf{r}_2\right)^{\mathrm{T}} \mathbf{Q}_{22}\left(\mathbf{z}_2 - \mathbf{r}_2\right) + \boldsymbol{\lambda}_1{}^{\mathrm{T}}(\dot{\mathbf{z}}_1) \tag{2.81}$$

And the costate vector, $\boldsymbol{\lambda}_1$ be expressed as,

$$\boldsymbol{\lambda}_1 = \Phi_1 \mathbf{z}_1 + \Psi_1 \tag{2.82}$$

Notice that,

$$\dot{\mathbf{z}}_1 = \mathbf{A}_{z11}\mathbf{z}_1 + \mathbf{A}_{z12}\mathbf{z}_2 + \mathbf{f}_{\mathbf{1z}} \tag{2.83}$$

Then, **H** becomes

$$\mathbf{H} = \frac{1}{2}\left(\mathbf{z}_1 - \mathbf{r}_1\right)^{\mathrm{T}} \mathbf{Q}_{11}\left(\mathbf{z}_1 - \mathbf{r}_1\right) + \frac{1}{2}\left(\mathbf{z}_2 - \mathbf{r}_2\right)^{\mathrm{T}} \mathbf{Q}_{22}\left(\mathbf{z}_2 - \mathbf{r}_2\right) + \boldsymbol{\lambda}_1{}^{\mathrm{T}}(\mathbf{A}_{z11}\mathbf{z}_1 + \mathbf{A}_{z12}\mathbf{z}_2 + \mathbf{f}_{\mathbf{1z}}) \tag{2.84}$$

By taking the relevant partial derivatives, the following equations are obtained.

$$\partial \mathbf{H} / \partial \mathbf{z}_2 = 0 \tag{2.85}$$

$$\partial \mathbf{H} / \partial \mathbf{z}_2 = \mathbf{Q}_{22}\left(\mathbf{z}_2 - \mathbf{r}_2\right) + \mathbf{A}_{z12}{}^{\mathrm{T}}\boldsymbol{\lambda}_1 = 0 \tag{2.86}$$

$$\dot{\mathbf{z}}_1 = \partial \mathbf{H} / \partial \boldsymbol{\lambda}_1 \tag{2.87}$$

$$\dot{\mathbf{z}}_1 = \mathbf{A}_{z11}\mathbf{z}_1 + \mathbf{A}_{z12}\left[\mathbf{r}_2 - \mathbf{Q}_{22}{}^{-1}\mathbf{A}_{z12}{}^{\mathrm{T}}\boldsymbol{\lambda}_1\right] + \mathbf{f}_{\mathbf{1z}} \tag{2.88}$$

$$\dot{\boldsymbol{\lambda}}_1 = -\partial \mathbf{H} / \partial \mathbf{z}_1 \tag{2.89}$$

$$\dot{\boldsymbol{\lambda}}_1 = -\mathbf{Q}_{11}\left(\mathbf{z}_1 - \mathbf{r}_1\right) - \mathbf{A}_{z11}{}^{\mathrm{T}}\boldsymbol{\lambda}_1 \tag{2.90}$$

By using the equation (2.86), the control structure can be expressed as follows,

$$\mathbf{z}_2 = \mathbf{r}_2 - \mathbf{Q}_{22}{}^{-1}\mathbf{A}_{z12}{}^{\mathrm{T}}\boldsymbol{\lambda}_1 \tag{2.91}$$

Finally equation (2.53), equation (2.90) and equation (2.91) can be combined as,

$$\mathbf{z}_2 = \mathbf{r}_2 - \mathbf{Q}_{22}{}^{-1}\mathbf{A}_{z12}{}^{\mathrm{T}}\Phi_1\mathbf{z}_1 - \mathbf{Q}_{22}{}^{-1}\mathbf{A}_{z12}{}^{\mathrm{T}}\Psi_1 = -\mathbf{C}\mathbf{z}_1 + \mathbf{h_2} \tag{2.92}$$

Hence, the slope $\mathbf{C}$ and offset of the sliding surface $\mathbf{h_2}$ can be defined as follows.

$$\mathbf{C} = \mathbf{Q}_{22}{}^{-1}\mathbf{A}_{z12}{}^{\mathrm{T}}\Phi_1 \tag{2.93}$$

$$\mathbf{h_2} = \mathbf{r}_2 - \mathbf{Q}_{22}{}^{-1}\mathbf{A}_{z12}{}^{\mathrm{T}}\Psi_1 \tag{2.94}$$

Then,

$$\boldsymbol{\lambda}_1 = \Phi_1\mathbf{z}_1 + \Psi_1 \Rightarrow \dot{\boldsymbol{\lambda}}_1 = \dot{\Phi}_1\mathbf{z}_1 + \Phi_1\dot{\mathbf{z}}_1 + \dot{\Psi}_1 \tag{2.95}$$

The final equation is derived by combining Equations (2.90) and (2.95). That is,

$$\dot{\boldsymbol{\lambda}}_1 = -\mathbf{Q}_{11}\left(\mathbf{z}_1 - \mathbf{r}_1\right) - \mathbf{A}_{z11}{}^{\mathrm{T}}\boldsymbol{\lambda}_1 = \dot{\Phi}_1\mathbf{z}_1 + \Phi_1\dot{\mathbf{z}}_1 + \dot{\Psi}_1 \tag{2.96}$$

This equation implies that

$$
\begin{aligned}
&-\mathbf{Q}_{11}\left(\mathbf{z}_1-\mathbf{r}_1\right)-\mathbf{A}_{z11}{}^{\mathrm{T}}\left(\Phi_1\mathbf{z}_1+\Psi_1\right)\\
&=\dot{\Phi}_1\mathbf{z}_1+\Phi_1\left(\mathbf{A}_{z11}\mathbf{z}_1+\mathbf{A}_{z12}\mathbf{r}_2-\mathbf{A}_{z12}\mathbf{Q}_{22}{}^{-1}\mathbf{A}_{z12}{}^{\mathrm{T}}\left[\Phi_1\mathbf{z}_1+\Psi_1\right]+\mathbf{f}_{\mathbf{1z}}\right)+\dot{\Psi}_1
\end{aligned}
\tag{2.97}
$$

By equating the coefficients of $\mathbf{z}_1$, the following two equations can be obtained;

$$
-\mathbf{Q}_{11}-\mathbf{A}_{z11}{}^{\mathrm{T}}\Phi_1=\dot{\Phi}_1\mathbf{z}_1+\Phi_1\mathbf{A}_{z11}-\Phi_1\mathbf{A}_{z12}\mathbf{Q}_{22}{}^{-1}\mathbf{A}_{z12}{}^{\mathrm{T}}\Phi_1 \tag{2.98}
$$

$$
\mathbf{Q}_{11}\mathbf{r}_1-\mathbf{A}_{z11}{}^{\mathrm{T}}\Psi_1=\Phi_1\mathbf{A}_{z12}\mathbf{r}_2-\Phi_1\mathbf{A}_{z12}\mathbf{Q}_{22}{}^{-1}\mathbf{A}_{z12}{}^{\mathrm{T}}\boldsymbol{\lambda}_1\Psi_1+\Phi_1\mathbf{f}_{\mathbf{1z}}+\dot{\Psi}_1 \tag{2.99}
$$

The above equations are solved for the steady state conditions by taking the derivatives equal to zero.

The first equation leads simply to the following algebraic matrix Riccati equation,

$$
\Phi_1\mathbf{A}_{z11}+\mathbf{A}_{z11}{}^{\mathrm{T}}\Phi_1-\Phi_1\mathbf{A}_{z12}\mathbf{Q}_{22}{}^{-1}\mathbf{A}_{z12}{}^{\mathrm{T}}\Phi_1+\mathbf{Q}_{11}=0 \tag{2.100}
$$

This equation is solved for Φ_1.

The steady state form of the second equation is

$$
\mathbf{Q}_{11}\mathbf{r}_1-\mathbf{A}_{z11}{}^{\mathrm{T}}\Psi_1=\Phi_1\mathbf{A}_{z12}\mathbf{r}_2-\Phi_1\mathbf{A}_{z12}\mathbf{Q}_{22}{}^{-1}\mathbf{A}_{z12}{}^{\mathrm{T}}\Psi_1+\Phi_1\mathbf{f}_{\mathbf{1z}} \tag{2.101}
$$

This equation can be rearranged as

$$\left(-\mathbf{A}_{z11}{}^{\mathrm{T}} + \Phi_1 \mathbf{A}_{z12} \mathbf{Q}_{22}{}^{-1} \mathbf{A}_{z12}{}^{\mathrm{T}}\right) \Psi_1 = -\mathbf{Q}_{11} \mathbf{r}_1 + \Phi_1 \left(\mathbf{A}_{z12} \mathbf{r}_2 + \mathbf{f}_{\mathbf{1z}}\right) \tag{2.102}$$

Hence, Ψ_1 is found as follows.

$$\Psi_1 = \left(-\mathbf{A}_{z11}{}^{\mathrm{T}} + \Phi_1 \mathbf{A}_{z12} \mathbf{Q}_{22}{}^{-1} \mathbf{A}_{z12}{}^{\mathrm{T}}\right)^{-1} \left(-\mathbf{Q}_{11} \mathbf{r}_1 + \Phi_1 \left[\mathbf{A}_{z12} \mathbf{r}_2 + \mathbf{f}_{\mathbf{1z}}\right]\right) \tag{2.103}$$

Since Φ_1 and Ψ_1 are known, the slope and the offset of the sliding surface can be determined as shown below.

$$\mathbf{C} = \mathbf{Q}_{22}{}^{-1} \mathbf{A}_{z12}{}^{\mathrm{T}} \Phi_1 \tag{2.104}$$

$$\mathbf{h_2} = \mathbf{r}_2 - \mathbf{Q}_{22}{}^{-1} \mathbf{A}_{z12}{}^{\mathrm{T}} \Psi_1 \tag{2.105}$$

The sliding mode controller is designed with a moving sliding surface such that its parameters, sliding surface slope and the offset of sliding surface, are determined in an adaptive manner and optimally selected for the given weighting matrix, $\mathbf{Q}$. In other words, sliding surface slope $\mathbf{C}$ and the offset of sliding surface $\mathbf{h_2}$ are determined and sliding mode controller can be derived using the equations (2.74), (2.75) and (2.76).

The use of "sign" function may yields numerical errors as a result of the insufficient integration time step selection during numerical calculations. Furthermore, because of the discontinuity across the sliding surfaces, the preceding control law may result in control chattering. As a practical matter, chattering is undesirable because it involves high frequency switched control action and may excite high frequency dynamics neglected in the modelling.

Therefore, to minimise these drawbacks, tangent hyperbolic function is used instead of sign function in the case study simulations. Thus, the following form is used in the case study simulations.

$$\mathbf{u}_{sw} = -\mathbf{B}_2^{-1}\mathbf{K}\begin{bmatrix} c_1 \tanh(\sigma_1) \\ c_2 \tanh(\sigma_2) \end{bmatrix} \tag{2.106}$$

where c_1 and c_2 are the parameters used to adjust the slope of the tangent hyperbolic function.

2.2.2 Pure SDRE Method

After the system dynamics is expressed in the form given by Equation (2.29), instead of designing a sliding mode controller, an ordinary feedback controller may also be designed. This controller is considered here for the sake of comparison with the SDRE-based SMC. Proposed SDRE-based SMC can also be compared different cases such as the SMC designed for the model linearised about the initial and/or final conditions or the SMC designed with constant sliding surface parameters i.e., the sliding surface slope and the offset of sliding surface. The reason why pure SDRE method, which the derivation is explained below, is selected as a comparision criteria for the proposed SDRE-based SMC is that; it is obvious that proposed SDRE-based SMC have much more better performances compared with the above two cases. But it is not as easy to say the same for the pure SDRE method without doing a case study.

The gain and the bias term of this feedback controller can again be determined by means of solving the State Dependent Riccati Equations. This means that the parameters of the ordinary feedback controller are also adapted in the same manner with those of the sliding mode controller.

In order to design this controller, the cost functional is taken as

$$J = \frac{1}{2}\int_0^\infty \left[\left(\tilde{\mathbf{x}} - \tilde{\mathbf{x}}_\mathrm{d}\right)^\mathrm{T} \mathbf{Q} \left(\tilde{\mathbf{x}} - \tilde{\mathbf{x}}_\mathrm{d}\right) + \mathbf{u}^\mathrm{T}\mathbf{R}\mathbf{u} \right] \mathrm{dt} \tag{2.107}$$

The control input can be expressed as

$$\mathbf{u} = -\mathbf{G}\tilde{\mathbf{x}} + \mathbf{b} \tag{2.108}$$

Here, $\mathbf{G}$ represents the gain of the feedback controller while $\mathbf{b}$ represents the bias term.

Hamiltonian is defined as

$$\mathbf{H} = \frac{1}{2}\left(\tilde{\mathbf{x}} - \tilde{\mathbf{x}}_{\mathrm{d}}\right)^{\mathrm{T}} \mathbf{Q}\left(\tilde{\mathbf{x}} - \tilde{\mathbf{x}}_{\mathrm{d}}\right) + \frac{1}{2}\mathbf{u}^{\mathrm{T}}\mathbf{R}\mathbf{u} + \boldsymbol{\lambda}_1{}^{\mathrm{T}}(\dot{\tilde{\mathbf{x}}}) \tag{2.109}$$

Note that,

$$\dot{\tilde{\mathbf{x}}} = \mathbf{A}(\tilde{\mathbf{x}})\tilde{\mathbf{x}} + \mathbf{B}(\tilde{\mathbf{x}})\mathbf{u} + \mathbf{f}(\tilde{\mathbf{x}}) + \mathbf{d}(\tilde{\mathbf{x}}) \tag{2.110}$$

The unknown disturbance term $\mathbf{d}(\tilde{\mathbf{x}})$ is not taken into account in the design of this controller. So,

$$\mathbf{H} = \frac{1}{2}\left(\tilde{\mathbf{x}} - \tilde{\mathbf{x}}_{\mathrm{d}}\right)^{\mathrm{T}} \mathbf{Q}\left(\tilde{\mathbf{x}} - \tilde{\mathbf{x}}_{\mathrm{d}}\right) + \frac{1}{2}\mathbf{u}^{\mathrm{T}}\mathbf{R}\mathbf{u} + \boldsymbol{\lambda}_1{}^{\mathrm{T}}\left[\mathbf{A}(\tilde{\mathbf{x}})\tilde{\mathbf{x}} + \mathbf{B}(\tilde{\mathbf{x}})\mathbf{u} + \mathbf{f}(\tilde{\mathbf{x}})\right] \tag{2.111}$$

However, as may be recalled, $\mathbf{d}(\tilde{\mathbf{x}})$ was taken into account with the estimated upper bounds of its components in designing the switching control of SMC.

By taking the relevant partial derivatives, the following equations are obtained.

$$\partial\mathbf{H}/\partial\,\mathbf{u} = 0 \tag{2.112}$$

$$\partial\mathbf{H}/\partial\,\mathbf{u} = \mathbf{R}\mathbf{u} + \mathbf{B}^{\mathrm{T}}\boldsymbol{\lambda}_1 = 0 \tag{2.113}$$

$$\mathbf{u} = -\mathbf{R}^{-1}\mathbf{B}^{\mathrm{T}}\boldsymbol{\lambda}_1 \tag{2.114}$$

$$\dot{\tilde{\mathbf{x}}} = \partial \mathbf{H} / \partial \boldsymbol{\lambda}_1 \tag{2.115}$$

$$\dot{\tilde{\mathbf{x}}} = \mathbf{A}\tilde{\mathbf{x}} + \mathbf{B}\left[-\mathbf{R}^{-1}\mathbf{B}^{\mathrm{T}}\boldsymbol{\lambda}_1\right] + \mathbf{f}(\tilde{\mathbf{x}}) \tag{2.116}$$

$$\dot{\boldsymbol{\lambda}}_1 = -\partial \mathbf{H} / \partial \dot{\tilde{\mathbf{x}}} \tag{2.117}$$

$$\dot{\boldsymbol{\lambda}}_1 = -\mathbf{Q}\left(\tilde{\mathbf{x}} - \tilde{\mathbf{x}}_{\mathrm{d}}\right) - \mathbf{A}^{\mathrm{T}}\boldsymbol{\lambda}_1 \tag{2.118}$$

Let costate vector be expressed as in (2.82),

$$\boldsymbol{\lambda}_1 = \Phi_1\tilde{\mathbf{x}} + \Psi_1$$

The derivative of the costate vector is as follows,

$$\dot{\boldsymbol{\lambda}}_1 = \dot{\Phi}_1\tilde{\mathbf{x}} + \Phi_1\dot{\tilde{\mathbf{x}}} + \dot{\Psi}_1 \tag{2.119}$$

Then the equations (2.117) and (2.119) are combined as

$$\dot{\boldsymbol{\lambda}}_1 = -\mathbf{Q}\left(\tilde{\mathbf{x}} - \tilde{\mathbf{x}}_{\mathrm{d}}\right) - \mathbf{A}^{\mathrm{T}}\left(\Phi_1\tilde{\mathbf{x}} + \Psi_1\right) = \dot{\Phi}_1\tilde{\mathbf{x}} + \Phi_1\left[\mathbf{A}\tilde{\mathbf{x}} + \mathbf{B}\left(-\mathbf{R}^{-1}\mathbf{B}^{\mathrm{T}}\boldsymbol{\lambda}_1\right) + \mathbf{f}(\tilde{\mathbf{x}})\right] + \dot{\Psi}_1 \tag{2.120}$$

By equating the coefficients of the $\tilde{\mathbf{x}}$, the following two equations are obtained.

$$-\mathbf{Q} - \mathbf{A}^{\mathrm{T}}\Phi_1 = \dot{\Phi}_1 + \Phi_1\mathbf{A} - \Phi_1\mathbf{B}\mathbf{R}^{-1}\mathbf{B}^{\mathrm{T}}\Phi_1 \tag{2.121}$$

$$\mathbf{Q}\tilde{\mathbf{x}}_d - \mathbf{A}^T\Psi_1 = -\Phi_1\mathbf{B}\mathbf{R}^{-1}\mathbf{B}^T\Psi_1 + \Phi_1\mathbf{f}\left(\tilde{\mathbf{x}}\right) + \dot{\Psi}_1 \tag{2.122}$$

The above equations are solved for the steady state conditions by taking the derivatives equal to zero. The first equation leads simply to the following algebraic matrix Riccati equation,

$$\Phi_1\mathbf{A} + \mathbf{A}^T\Phi_1 - \Phi_1\mathbf{B}\mathbf{R}^{-1}\mathbf{B}^T\Phi_1 + \mathbf{Q} = 0 \tag{2.123}$$

This equation is solved for Φ_1.

The steady state form of the second equation is

$$\mathbf{Q}\tilde{\mathbf{x}}_d - \mathbf{A}^T\Psi_1 = -\Phi_1\mathbf{B}\mathbf{R}^{-1}\mathbf{B}^T\Psi_1 + \Phi_1\mathbf{f}\left(\tilde{\mathbf{x}}\right) \tag{2.124}$$

This equation can be solved for Ψ_1 as

$$\Psi_1 = \left(-\mathbf{A}^T + \Phi_1\mathbf{B}\mathbf{R}^{-1}\mathbf{B}^T\right)^{-1}\left(-\mathbf{Q}\tilde{\mathbf{x}}_d + \Phi_1\mathbf{f}\left(\tilde{\mathbf{x}}\right)\right) \tag{2.125}$$

Since Φ_1 and Ψ_1 are known, the gain of the feedback controller and the bias term can be determined by combining the equations (2.108) and (2.114) so that,

$$\mathbf{G} = \mathbf{R}^{-1}\mathbf{B}^T\Phi_1 \tag{2.126}$$

$$\mathbf{b} = -\mathbf{R}^{-1}\mathbf{B}^T\Psi_1 \tag{2.127}$$

CHAPTER 3

APPLICATION OF THE DESIGNED CONTROLLER TO A HYPERSONIC AIR VEHICLE MODEL

This section includes the application of the proposed adaptive SMC to the generic hypersonic vehicle model which was also studied in the main reference article [10] and the result of the case study simulations. This case study example is used mainly for comparison purposes with an alternative adaptive SMC applied to the same vehicle in [10]. The units used in the case study simulations are kept same with the ones in [10] during plotting phase to allow us to compare the results.

3.1 Mathematical Model of the Hypersonic Air Vehicle

The model which was also studied in the main reference article [10] is used in this thesis study.

3.1.1 Nomenclature

A	Speed of Sound, m/s (ft/s)
C_D	Drag Coefficient
C_L	Lift Coefficient
$C_M(q)$	Moment Coefficient due to Pitch Rate
$C_M(\alpha)$	Moment Coefficient due to Angle of Attack
$C_M(\delta_e)$	Moment Coefficient due to Elevator Deflection
C_T	Thrust Coefficient
C	Reference Length, 24.4 m (80 ft)
D	Drag, N (lbf)
h	Altitude, m (ft)
I_{yy}	Moment of Inertia, 9.5 x10^6 kg-m^2 (7x10^6 slug-ft^2)

L	Lift, N (lbf)
M	Mach Number
M_{yy}	Pitching Moment, N.m (lbf-ft)
m	Mass, 136818 kg (9375 slugs)
q	Pitch Rate, rad/s
R_E	Radius of the Earth, 6371400 m (20903500 ft)
r	Radial Distance from Earth's center, m (ft)
S	Reference Area, 335 m^2 (3603 ft^2)
T	Thrust, N (lbf)
V	Velocity, m/s (ft/s)
α	Angle of Attack, rad
β	Throttle Setting
γ	Flight-Path Angle, rad
δ_e	Elevator Deflection, rad
μ	Gravitational Constant , 3.94 x10^{14} m^3/s^2 (1.39x10^{16} ft^3/s^2)
ρ	Density of Air, 0.013 kg/m^3 (0.24325x10^{-4} slugs/ft^3)

3.1.2 Differential Equations of the System

A simplified version of the model used in [12] and [15] has been presented in [10]. The model describing the longitudinal dynamics of a generic hypersonic air vehicle has been simplified by making appropriate modifications for the trimmed cruise condition (M=15, V=4,590 m/s (15,060 ft/s), h=33,528 m (110,000 ft), γ=0 deg, and q=0 deg/s). The equations of motions derived for this vehicle include an inverse-square-law gravitational model, and the centripetal acceleration for the nonrotating Earth.

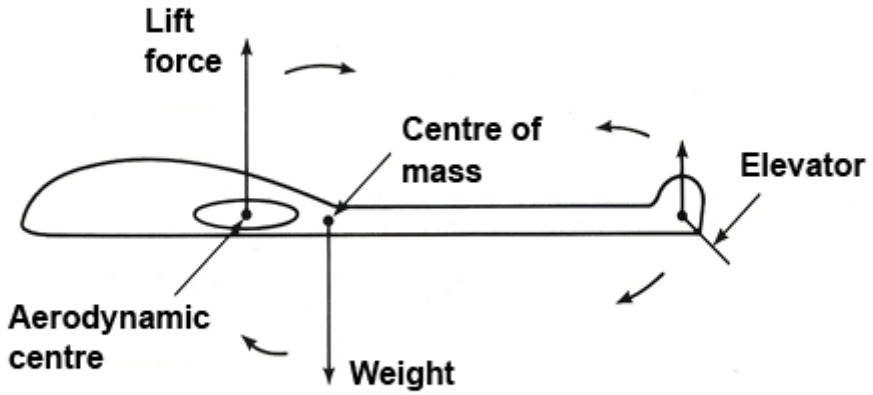

Figure 3.1 Free Body Diagram of a Simplified Hypersonic Air Vehicle
(Resource: Adaptive Predictive Expert Control, [14])

The equations of motion for the hypersonic air vehicle model are given below:

$$\dot{V} = \frac{T\cos\alpha - D}{m} - \frac{\mu\sin\gamma}{r^2} \tag{3.1}$$

$$\dot{\gamma} = \frac{L+T\sin\alpha}{mV} - \frac{\left(\mu - V^2 r\right)\cos\gamma}{Vr^2} \tag{3.2}$$

$$\dot{h} = V\sin\gamma \tag{3.3}$$

$$a = q - \dot{\gamma} \tag{3.4}$$

$$\dot{q} = M_{yy} / I_{yy} \tag{3.5}$$

where

$$L = \frac{1}{2}\rho V^2 S C_L \tag{3.6}$$

$$D = \frac{1}{2}\rho V^2 S C_D \tag{3.7}$$

$$T = \frac{1}{2}\rho V^2 S C_T \tag{3.8}$$

$$M_{yy} = \frac{1}{2}\rho V^2 S\bar{c}\left[C_M(\alpha)+C_M(\delta_e)+C_M(q)\right] \tag{3.9}$$

$$r = h+R_E \tag{3.10}$$

$$C_L = 0.6203\alpha \tag{3.11}$$

$$C_D = 0.6450\alpha^2+0.0043378\alpha+0.003772 \tag{3.12}$$

$$C_T = \begin{cases} 0.02576\beta, & (\beta<1) \\ 0.02240 + 0.00336\beta, & (\beta>1) \end{cases} \tag{3.13}$$

$$C_M(\alpha) = -0.035\alpha^2 + 0.036617\alpha + 5.3261\times10^{-6} \tag{3.14}$$

$$C_M(q) = \left(\bar{c}/2V\right) q(-6.796\alpha^2 + 0.3015\alpha - 0.2289) \tag{3.15}$$

$$C_M(\delta_e) = c_e\left(\delta_e - \alpha\right) \tag{3.16}$$

where it is assumed that c_e remains constant as $c_e = 0.0292$.

3.2 Sliding Mode Control Design for the Hypersonic Air Vehicle Model

The hypersonic air vehicle can be modelled as follows.

$$\dot{\mathbf{x}} = \mathbf{a(x)} + \mathbf{B(x)u} \tag{3.17}$$

where

$$\dot{\mathbf{x}} = \begin{bmatrix} \dot{x}_1 \\ \dot{x}_2 \\ \dot{x}_3 \\ \dot{x}_4 \\ \dot{x}_5 \end{bmatrix} = \begin{bmatrix} \dot{V} \\ \dot{\gamma} \\ \dot{h} \\ \dot{\alpha} \\ \dot{q} \end{bmatrix} \quad \text{and,} \tag{3.18}$$

$$\mathbf{u} = \begin{bmatrix} u_1 \\ u_2 \end{bmatrix} = \begin{bmatrix} \delta_e \\ \beta \end{bmatrix} \tag{3.19}$$

By rearranging the differential equations of the system, it is seen that

$$\mathbf{a(x)} = \begin{bmatrix} \dfrac{-\rho S x_1^{\,2}}{2m}\left\{(0.6450x_4^{\,2}+0.0043378x_4+0.003772)-\dfrac{\mu \sin x_2}{(x_3+R_e)^2}\right\} \\ \dfrac{\rho S x_1}{2m}\left\{0.6203x_4-\dfrac{\left(\mu-x_1^{\,2}\{x_3+R_e\}\right)\cos x_2}{x_1(x_3+R_e)^2}\right\} \\ x_1 \sin x_2 \\ x_5-\left\{\dfrac{\rho S x_1}{2m}\left(0.6203x_4-\dfrac{\left(\mu-x_1^{\,2}\right)(x_3+R_e)\cos x_2}{x_1(x_3+R_e)^2}\right)\right\} \\ \dfrac{\rho S x_1^{\,2}\bar{c}}{2I_{yy}}\left\{(-0.035x_4^{\,2}+(0.036617-c_e)x_4+5.3261\mathrm{e}^{-6})+\dfrac{\bar{c}}{2x_1}x_5(-6.796x_4^{\,2}+0.3015x_4-0.2289)\right\} \end{bmatrix} \tag{3.20}$$

$$\mathbf{B(x)} = \begin{bmatrix} 0 & \frac{\rho S x_1^{\,2}}{2m}\left(0.02576\cos x_4\right) \\ 0 & \frac{\rho S x_1}{2m}\left(0.02576\sin x_4\right) \\ 0 & 0 \\ 0 & \frac{-\rho S x_1^{\,2}}{2m}\left(0.02576\cos x_4\right) \\ \frac{\rho S x_1^{\,2}\bar{c}c_e}{2I_{yy}} & 0 \end{bmatrix} \tag{3.21}$$

However, the state equation of the system that is going to be controlled with this methodology should be in the following form:

$$\dot{\mathbf{x}} = \mathbf{A}(\mathbf{x})\mathbf{x} + \mathbf{B}(\mathbf{x})\mathbf{u} + \mathbf{d}(\mathbf{x}) \tag{3.22}$$

In this study, the required form is obtained as follows for the hypersonic air vehicle.

$$\dot{\tilde{\mathbf{x}}} = \mathbf{A}(\tilde{\mathbf{x}})\tilde{\mathbf{x}} + \mathbf{B}(\tilde{\mathbf{x}})\mathbf{u} + \mathbf{f}(\tilde{\mathbf{x}}) + \mathbf{d}(\tilde{\mathbf{x}}) \tag{3.23}$$

where

$$\tilde{\mathbf{x}} = \begin{bmatrix} \tilde{x}_1 \\ x_2 \\ \tilde{x}_3 \\ x_4 \\ x_5 \end{bmatrix} = \begin{bmatrix} \tilde{V} \\ \gamma \\ \tilde{h} \\ \alpha \\ q \end{bmatrix} \text{ and, } \mathbf{u} = \begin{bmatrix} u_1 \\ u_2 \end{bmatrix} = \begin{bmatrix} \delta_e \\ \beta \end{bmatrix} \tag{3.24}$$

By rearranging the differential equations of the system, the following set of equations can be obtained,

$$\dot{x}_1 = \underbrace{\left(-\frac{\rho S x_1}{2m}\left[0.003772\right]\right)}_{a_{11}} x_1 + \underbrace{\left(-\frac{\mu \sin x_2}{x_2 (x_3 + R_e)^2}\right)}_{a_{12}} x_2$$
$$+ \underbrace{\left(\frac{-\rho S x_1^{\,2}}{2m}\left[0.6450 x_4 + 0.0043378\right]\right)}_{a_{14}} x_4 + \underbrace{\left(\frac{\rho S x_1^{\,2}}{2m}\left[\left(0.02576 \cos x_4\right)\right]\right)}_{b_{12}} u_2 \tag{3.25}$$

$$\dot{x}_2 = \underbrace{\left(-\frac{\left[\mu - x_1^{\,2}\left\{x_3 + R_e\right\}\right]\cos x_2}{x_1^{\,2}(x_3 + R_e)^2}\right)}_{a_{21}} x_1 + \underbrace{\left(\frac{\rho S x_1}{2m}\left[0.6203\right]\right)}_{a_{24}} x_4$$
$$+ \underbrace{\left(\frac{\rho S x_1}{2m}\left[\left(0.02576 \sin x_4\right)\right]\right)}_{b_{22}} u_2 \tag{3.26}$$

$$\dot{x}_3 = \underbrace{\left(x_1 \frac{\sin x_2}{x_2}\right)}_{a_{32}} x_2 \tag{3.27}$$

$$\dot{x}_4 = \underbrace{\left(\frac{\left[\mu - \mathrm{x}_1^{\,2}\left\{x_3 + R_e\right\}\right]\cos x_2}{x_1^{\,2}(x_3 + R_e)^2}\right)}_{a_{41}} x_1 + \underbrace{\left(-\frac{\rho S x_1}{2m}\left[0.6203\right]\right)}_{a_{44}} x_4 + x_5$$
$$+ \underbrace{\left(-\frac{\rho S x_1}{2m}\left[\left(0.02576 \sin x_4\right)\right]\right)}_{b_{42}} u_2 \tag{3.28}$$

$$\dot{x}_5 = \underbrace{\left(\frac{\rho S x_1 \bar{c}}{2I_{yy}} \left[5.3261\mathrm{e}^{-6} \right] \right)}_{a_{51}} x_1$$

$$+ \underbrace{\left(\left\{ \frac{\rho S x_1{}^2 \bar{c}}{2I_{yy}} \left[-0.035x_4 + 0.036617 - c_e \right] \right\} + \left\{ \frac{\rho S x_1 \bar{c}^2 x_5}{4I_{yy}} \left[-6.796x_4 + 0.3015 \right] \right\} \right)}_{a_{54}} x_4$$

$$+ \underbrace{\left(-\frac{\rho S x_1 \bar{c}^2}{4I_{yy}} \left[0.2289 \right] \right)}_{a_{55}} x_5 + \underbrace{\left(\frac{\rho S x_1{}^2 \bar{c}}{2I_{yy}} \left[c_e \right] \right)}_{b_{51}} u_2 \tag{3.29}$$

The arrangements made above in order to obtain the state dependent coefficients are of course not unique. Here, the arrangement is preferred to be such that the system state variables which are physically changing in a relatively fast manner such as the angle of attack, the flight path angle and the pitch rate are factored out as linear multipliers of the state dependent coefficients a_{ij} (i, j = 1 to 5).

One of the factors that the performance of the controller over the domain of interest is state dependent coefficient (SDC) matrix $\mathbf{A}(\mathbf{x})$. In the multivariable case, the SDC parameterisation is not unique and there is no systematic way to express $\mathbf{a}(\mathbf{x})$ as $\mathbf{A}(\mathbf{x})\mathbf{x}$. By definition, the pair $\{\mathbf{A}(\mathbf{x}), \mathbf{B}(\mathbf{x})\}$ is a controllable (stabilisable) parameterisation of the nonlinear system in a region Ω if $\{\mathbf{A}(\mathbf{x}), \mathbf{B}(\mathbf{x})\}$ is pointwise controllable (stabilisable) in the linear sense for all $\mathbf{x} \in \Omega$. This definition is used to guarantee that the SDRE nonlinear regulator produces a closed-loop solution which is locally asymptotically stable [15].

In this case study, the pointwise controllability of the pair $\{\mathbf{A}(\mathbf{x}), \mathbf{B}(\mathbf{x})\}$ is checked at each time increment during simulations. A special simulation is performed to observe the pointwise controllability for the whole simulation duration and it is seen that pointwise controllability criteria is satisfied.

As a summary, the following state-space representation is obtained.

$$\dot{\mathbf{x}} = \begin{bmatrix} \dot{x}_1 \\ \dot{x}_2 \\ \dot{x}_3 \\ \dot{x}_4 \\ \dot{x}_5 \end{bmatrix} = \underbrace{\begin{bmatrix} a_{11} & a_{12} & 0 & a_{14} & 0 \\ a_{21} & 0 & 0 & a_{24} & 0 \\ 0 & a_{32} & 0 & 0 & 0 \\ a_{41} & 0 & 0 & a_{44} & 1 \\ a_{51} & 0 & 0 & a_{54} & a_{55} \end{bmatrix}}_{\mathbf{A(x)}} \mathbf{x} + \underbrace{\begin{bmatrix} 0 & b_{12} \\ 0 & b_{22} \\ 0 & 0 \\ 0 & b_{42} \\ b_{51} & 0 \end{bmatrix}}_{\mathbf{B(x)}} \mathbf{u} \tag{3.30}$$

Here, the state variables are the percentage change in the velocity relative to its initial condition, the flight path angle, the percentage change in the altitude relative to its initial condition, the angle of attack and the pitch rate.

Percentage changes of the velocity and altitude are used as the first and third state variables in order to make all the state variables have comparable orders of magnitude.

Otherwise, the difference between the order of the first and third system state variables and the remaining ones lead to computational difficulties. These percentage changes are defined as follows.

$$\tilde{V} = \frac{V - V_0}{V_0} \Rightarrow \tilde{x}_1 = \frac{x_1 - x_{10}}{x_{10}} \tag{3.31}$$

therefore,

$$x_1 = x_{10}\left(1+\tilde{x}_1\right) \tag{3.32}$$

and,

$$\dot{x}_1 = \dot{\tilde{x}}_1 x_{10} \tag{3.33}$$

$$\tilde{h} = \frac{h - h_0}{h_0} \Rightarrow \tilde{\mathrm{x}}_3 = \frac{x_3 - x_{30}}{x_{30}} \tag{3.34}$$

therefore,

$$x_3 = x_{30}\left(1+\tilde{x}_3\right) \tag{3.35}$$

and,

$$\dot{x}_3 = \dot{\tilde{x}}_3 x_{30} \tag{3.36}$$

As the next step, the change in first and third system state variables in terms of percentage change relative to their initial conditions are reflected to the above state space representation in Eqn. (3.30). The following equations are obtained,

$$\dot{\tilde{x}}_1 = \frac{\dot{x}_1}{x_{10}} = \frac{a_{11}x_1 + a_{12}x_2 + a_{14}x_4 + b_{12}u_2}{x_{10}}; \tag{3.37}$$

$$x_1 = x_{10}\left(1+\tilde{x}_1\right) \tag{3.38}$$

$$x_3 = x_{30}\left(1+\tilde{x}_3\right) \tag{3.39}$$

$$\dot{\tilde{x}}_1 = \frac{\dot{x}_1}{x_{10}} = \frac{a_{11}\left[x_{10}\left(1+\tilde{x}_1\right)\right] + a_{12}x_2 + a_{14}x_4 + b_{12}u_2}{x_{10}} \tag{3.40}$$

$$\dot{\tilde{x}}_1 = a_{11} + a_{11}\tilde{x}_1 + \frac{a_{12}}{x_{10}}x_2 + \frac{a_{14}}{x_{10}}x_4 + \frac{b_{12}}{x_{10}}u_2 \tag{3.41}$$

$$\dot{x}_2 = a_{21}x_1 + a_{24}x_4 + b_{22}u_2; \tag{3.42}$$

$$x_1 = x_{10}\left(1+\tilde{x}_1\right) \tag{3.43}$$

$$x_3 = x_{30}\left(1+\tilde{x}_3\right) \tag{3.44}$$

$$\dot{x}_2 = a_{21}\left[x_{10}\left(1+\tilde{x}_1\right)\right] + a_{24}x_4 + b_{22}u_2 \tag{3.45}$$

$$\dot{x}_2 = a_{21}x_{10} + \left(a_{21}x_{10}\right)\tilde{x}_1 + a_{24}x_4 + b_{22}u_2 \tag{3.46}$$

$$\dot{\tilde{x}}_3 = \frac{\dot{x}_3}{x_{30}} = \frac{\dot{x}_3}{x_{30}} = \frac{a_{32}x_2}{x_{30}} = \frac{a_{32}}{x_{30}}x_2 \tag{3.47}$$

$$\dot{x}_4 = a_{41}x_1 + a_{44}x_4 + x_5 + b_{42}u_2; \tag{3.48}$$

$$x_1 = x_{10}\left(1+\tilde{x}_1\right) \tag{3.49}$$

$$x_3 = x_{30}\left(1+\tilde{x}_3\right) \tag{3.50}$$

$$\dot{x}_4 = a_{41}\left[x_{10}\left(1+\tilde{x}_1\right)\right] + a_{44}x_4 + x_5 + b_{42}u_2 \tag{3.51}$$

$$\dot{x}_4 = a_{41}x_{10} + \left(a_{41}x_{10}\right)\tilde{x}_1 + a_{24}x_4 + x_5 + b_{42}u_2 \tag{3.52}$$

$$\dot{x}_5 = a_{51}x_1 + a_{54}x_4 + a_{55}x_5 + b_{51}u_1; \tag{3.53}$$

$$x_1 = x_{10}\left(1+\tilde{x}_1\right) \tag{3.54}$$

$$x_3 = x_{30}\left(1+\tilde{x}_3\right) \tag{3.55}$$

$$\dot{x}_5 = a_{51}\left[x_{10}\left(1+\tilde{x}_1\right)\right] + a_{54}x_4 + a_{55}x_5 + b_{51}u_1 \tag{3.56}$$

$$\dot{x}_5 = a_{51}x_{10} + \left(a_{51}x_{10}\right)\tilde{x}_1 + a_{54}x_4 + a_{55}x_5 + b_{51}u_1 \tag{3.57}$$

Here, the state dependent coefficients a_{ij} (i, j = 1 to 5) are also re-calculated with the change of $x_1 = x_{10}\left(1+\tilde{x}_1\right)$ and $x_3 = x_{30}\left(1+\tilde{x}_3\right)$ but the same notation is used to prevent ambiguity. As an example,

$$a_{11} = -\frac{\rho S x_1}{2m}\left[0.003772\right] \tag{3.58}$$

and,

$$x_1 = x_{10}\left(1+\tilde{x}_1\right) \tag{3.59}$$

So the new a_{11} coefficient is determined as follows,

$$a_{11} = -\frac{\rho S\left\{x_{10}\left(1+\tilde{x}_1\right)\right\}}{2m}\left[0.003772\right] \tag{3.60}$$

The updated state space representation is as follows,

$$\dot{\tilde{\mathbf{x}}} = \begin{bmatrix} \dot{\tilde{x}}_1 \\ \dot{x}_2 \\ \dot{\tilde{x}}_3 \\ \dot{x}_4 \\ \dot{x}_5 \end{bmatrix} = \underbrace{\begin{bmatrix} a_{11} & a_{12}/x_{10} & 0 & a_{14}/x_{10} & 0 \\ a_{21}x_{10} & 0 & 0 & a_{24} & 0 \\ 0 & a_{32}/x_{30} & 0 & 0 & 0 \\ a_{41}x_{10} & 0 & 0 & a_{44} & 1 \\ a_{51}x_{10} & 0 & 0 & a_{54} & a_{55} \end{bmatrix}}_{\mathbf{A}(\tilde{\mathbf{x}})} \tilde{\mathbf{x}} + \underbrace{\begin{bmatrix} 0 & b_{12}/x_{10} \\ 0 & b_{22} \\ 0 & 0 \\ 0 & b_{42} \\ b_{51} & 0 \end{bmatrix}}_{\mathbf{B}(\tilde{\mathbf{x}})} \mathbf{u} + \underbrace{\begin{bmatrix} a_{11} \\ a_{21}x_{10} \\ 0 \\ a_{41}x_{10} \\ a_{51}x_{10} \end{bmatrix}}_{\mathbf{f}(\tilde{\mathbf{x}})} \tag{3.61}$$

It should be noted that the term $\mathbf{f}(\tilde{\mathbf{x}})$, appears in the updated system state representation as a result of this new definition of the first and third system state variables.

Lastly, the state dependent disturbance is added to the system. Disturbance is assumed as the wind effect which affects the related aerodynamic coefficients by changing the angle of attack of the aircraft relative to the wind. It is assumed that the disturbance effect is additive and affects only the angle of attack dependent aerodynamic coefficients: C_L, C_D and $C_M(a)$.

The additional disturbance terms are given below,

$$C_{Lw} = 0.6203\Delta\alpha_{\mathrm{w}} \tag{3.62}$$

$$C_{Dw} = 0.6450\Delta\alpha_{\mathrm{w}}{}^{2} + 0.0043378\Delta\alpha_{\mathrm{w}} + 0.003772 \tag{3.63}$$

$$C_{M_w}(\alpha) = -0.035\Delta\alpha_{\mathrm{w}}{}^{2} + 0.036617\Delta\alpha_{\mathrm{w}} + 5.3261\times10^{-6} \tag{3.64}$$

where,

$\Delta\alpha_{\mathrm{w}}$ is the additional angle of attack and equal to the difference between the aircraft angle of attack α and the angle of attack relative to the wind α_{w}. α_{w} is the result of the combination of the aircraft speed and wind speed while α is the aircraft angle of attack measured when there is no wind.

Additional angle of attack term is defined as a fluctuating signal around its non-zero mean value. The expression is as following,

$$\Delta\alpha_{\mathrm{w}} = \underbrace{-0.25^{\circ}}_{\Delta\alpha_{\mathrm{w1}}} + \underbrace{0.025^{\circ}\left(\sin t + \sin\left[\left(\sqrt{3}\right)t\right] + \sin\left[\left(\sqrt{5}\right)t\right]\right)}_{\Delta\alpha_{\mathrm{w2}}} \tag{3.65}$$

$$\Delta\alpha_{\mathrm{w1}} = -0.25^{\circ} \tag{3.66}$$

$$\Delta\alpha_{\mathrm{w2}} = 0.025^{\circ}\left(\sin t + \sin\left[\left(\sqrt{3}\right)t\right] + \sin\left[\left(\sqrt{5}\right)t\right]\right) \tag{3.67}$$

The expression in (3.65) is carefully selected to guarantee that harmonics and repeated terms are avoided. In other words, by injecting the irrational numbers into the sine functions, a mimicking random signal is generated for the computer simulations.

Lift and Drag forces and pitching moment are affected by the addition of these coefficients. Since,

$$L_w = \frac{1}{2}\rho V^2 S C_{Lw} \tag{3.68}$$

$$D_w = \frac{1}{2}\rho V^2 S C_{Dw} \tag{3.69}$$

$$M_{yy_w} = \frac{1}{2}\rho V^2 S\bar{c}\left[C_{M_w}(\alpha)\right] \tag{3.70}$$

The constant parts of the additional disturbance terms occurred as a result of the new lift and drag forces and pitching moment are embedded inside the system matrix $\mathbf{A}(\tilde{\mathbf{x}})$ and $\mathbf{f}(\tilde{\mathbf{x}})$ to guarantee that they can be compensated by the sliding mode controller. The fluctuating parts on the other hand are represented by the addition $\mathbf{d}(\tilde{\mathbf{x}})$ matrix to the state space representations. $\mathbf{d}(\tilde{\mathbf{x}})$ is given below,

$$\mathbf{d}(\tilde{\mathbf{x}}) = \begin{bmatrix} -\dfrac{\rho S\tilde{x}_1^{\,2}}{2mx_{10}}\left(0.6450\left(2\Delta\alpha_{w1}\Delta\alpha_{w2}\right)+0.6450\left(\Delta\alpha_{w2}\right)^2+0.0043378\Delta\alpha_{w2}\right) \\ \dfrac{\rho S\tilde{x}_1}{2m}\left(0.6203\Delta\alpha_{w2}\right) \\ 0 \\ -\dfrac{\rho S\tilde{x}_1}{2m}\left(0.6203\Delta\alpha_{w2}\right) \\ \dfrac{\rho S\tilde{x}_1^{\,2}\bar{c}}{2I_{yy}}\left(-0.035\left(2\Delta\alpha_{w1}\Delta\alpha_{w2}\right)-0.035\left(\Delta\alpha_{w2}\right)^2+0.036617\Delta\alpha_{w2}\right) \end{bmatrix} \tag{3.71}$$

So, the final state space form of the system can be shown as,

$$\dot{\mathbf{x}} = \mathbf{A}(\tilde{\mathbf{x}})\tilde{\mathbf{x}} + \mathbf{B}(\tilde{\mathbf{x}})\mathbf{u} + \mathbf{f}(\tilde{\mathbf{x}}) + \mathbf{d}(\tilde{\mathbf{x}}) \tag{3.72}$$

$$\dot{\tilde{\mathbf{x}}} = \begin{bmatrix} \dot{\tilde{x}}_1 \\ \dot{x}_2 \\ \dot{\tilde{x}}_3 \\ \dot{x}_4 \\ \dot{x}_5 \end{bmatrix} = \underbrace{\begin{bmatrix} 2a_{11} & a_{12}/x_{10} & 0 & a_{14}/x_{10} & 0 \\ a_{21}x_{10} & 0 & 0 & a_{24} & 0 \\ 0 & a_{32}/x_{30} & 0 & 0 & 0 \\ a_{41}x_{10} & 0 & 0 & a_{44} & 1 \\ 2a_{51}x_{10} & 0 & 0 & a_{54} & a_{55} \end{bmatrix}}_{\mathbf{A}(\tilde{\mathbf{x}})} \tilde{\mathbf{x}} + \underbrace{\begin{bmatrix} 0 & b_{12}/x_{10} \\ 0 & b_{22} \\ 0 & 0 \\ 0 & b_{42} \\ b_{51} & 0 \end{bmatrix}}_{\mathbf{B}(\mathbf{x})} \mathbf{u}$$

$$+ \underbrace{\begin{bmatrix} 2a_{11}+\left\{-\dfrac{\rho S\tilde{x}_1^{\,2}}{2mx_{10}}\left(0.6450\left(\Delta\alpha_{w1}\right)^2+0.0043378\Delta\alpha_{w1}\right)\right\} \\ a_{21}x_{10}+\left\{\dfrac{\rho S\tilde{x}_1}{2m}\left(0.6203\Delta\alpha_{w1}\right)\right\} \\ 0 \\ a_{41}x_{10}-\left\{\dfrac{\rho S\tilde{x}_1}{2m}\left(0.6203\Delta\alpha_{w1}\right)\right\} \\ 2a_{51}x_{10}+\left\{\dfrac{\rho S\tilde{x}_1^{\,2}\bar{c}}{2I_{yy}}\left(-0.035\left(\Delta\alpha_{w1}\right)^2+0.036617\Delta\alpha_{w1}\right)\right\} \end{bmatrix}}_{\mathbf{f}(\tilde{\mathbf{x}})}$$

$$+\underbrace{\begin{bmatrix} -\dfrac{\rho S\tilde{x}_1^{\,2}}{2mx_{10}}\left(0.6450\left(2\Delta\alpha_{w1}\Delta\alpha_{w2}\right)+0.6450\left(\Delta\alpha_{w2}\right)^2+0.0043378\Delta\alpha_{w2}\right) \\ \dfrac{\rho S\tilde{x}_1}{2m}\left(0.6203\Delta\alpha_{w2}\right) \\ 0 \\ -\dfrac{\rho S\tilde{x}_1}{2m}\left(0.6203\Delta\alpha_{w2}\right) \\ \dfrac{\rho S\tilde{x}_1^{\,2}\bar{c}}{2I_{yy}}\left(-0.035\left(2\Delta\alpha_{w1}\Delta\alpha_{w2}\right)-0.035\left(\Delta\alpha_{w2}\right)^2+0.036617\Delta\alpha_{w2}\right) \end{bmatrix}}_{\mathbf{d}(\tilde{\mathbf{x}})} \tag{3.73}$$

3.3 Computer Simulations for the Designed Controllers

To evaluate the performance of the designed controllers, system simulations have been accomplished by using MATLAB® (The MathWorks Inc., 2004) software. To create the simulations, some functions and scripts are built which use the system non-linear equations. These functions and scripts use the SMC design methodology described in section 2.2. The system is first transformed to the necessary state space form and then transformed to the so-called reduced order form. Sliding surface slope and the sliding surface offset parameters are determined by solving the SDRE's for the selected weighting matrices $\mathbf{Q_{11}}$ and $\mathbf{Q_{22}}$ at each change in system state variables as a next step. Before plotting the results, SMC is created as the sum of two components. Finally, "state variables", "control inputs", "deviation from the sliding surface", "sliding surface slope", "the sliding surface offset" and "disturbance variations" are plotted to evaluate the system performance. The notations "s" and "sec" are all used in this chapter to represent the time unit "second".

The differential equation inside the function is solved by modified version of the MATLAB®'s (The MathWorks Inc., 2004) special function "ode5" numerically. The modification allowed us to calculate the derivatives of transformation matrix, sliding surface slope and the sliding surface offset which are necessary for SMC design.

The MATLAB® (The MathWorks Inc., 2004) scripts and functions developed in this study are given in Appendices; Appendix A, Appendix B, Appendix C, Appendix D, Appendix E. A brief user manual can also be found in Appendix F.

It is required that the system to track 100 ft/s step velocity command and 2000 ft step altitude command together. In the simulations, the elements of control gain matrix **K** are selected as -0.002 and -0.0004 for first and second control inputs respectively.

Although it is possible to select different weighting matrices in the cost function (even state dependent weighting matrices), as a case study, the following weighting matrices are used in the simulations.

$$\mathbf{Q}_{11} = \begin{bmatrix} 3000 & 0 & 0 & 0 & 0 \\ 0 & 300 & 0 & 0 & 0 \\ 0 & 0 & 300 & 0 & 0 \\ 0 & 0 & 0 & 60 & 0 \\ 0 & 0 & 0 & 0 & 300 \end{bmatrix} \text{ and } \mathbf{Q}_{22} = \begin{bmatrix} 1 & 0 \\ 0 & 1 \end{bmatrix} \tag{3.74}$$

These weighting matrices are chosen from a set of simulation results in which stability of the closed loop system is assured.

To have a comparison, the pure SDRE technique is applied alone first and then the SMC method combined with SDRE is simulated. In both simulations, all the initial and desired state and control values are taken to be the same. The main difference between two methods is the design methodology of the controller. In the first one, simple feedback controller is applied, but the gains are still determined online during the control process according to the solutions of the SDRE's. In the second method, a sliding mode controller is designed for the same model which is capable of adapting the sliding surface online during the control process based on the solutions of the SDRE's.
The simulations have been performed for the nominal model and for the model under the presence of disturbances for both techniques.

While plotting the state variables, the first variable (velocity) and third state variable (altitude) are represented in terms of variations to see the ability of tracking the steps commands accurately. The other terms are kept as they are; in other words, they are represented in terms of real state variables and control inputs. The constants are given in section 3.1.1 and there is no need to repeat them here. Results of the computer simulations (for the designed controller with the initial and final conditions given below are presented in sections 3.3.1 and 3.3.2:

Simulations for 100 ft/s Velocity and 2000 ft Altitude Step Commands without Disturbance:

	Initial	Final (Desired)
Velocity	4590 m (15060 ft/s)	4620 m (15160 ft/s)
Flight Path Angle (deg)	0	0
Altitude (ft)	33528 m (110000 ft/s)	34137 m (112000 ft/s)
Angle of Attack (deg)	1.79	1.7530
Pitch Rate (deg/s)	0	0
Elevator Deflection (deg)	-	-0.3914
Throttle Setting	-	0.1751

Simulations for 100 ft/s Velocity and 2000 ft Altitude Step Commands Disturbance:

	Initial	Final (Desired)
Velocity	4590 m (15060 ft/s)	4620 m (15160 ft/s)
Flight Path Angle (deg)	0	0
Altitude (ft)	33528 m (110000 ft/s)	34137 m (112000 ft/s)
Angle of Attack (deg)	1.79	2.000
Pitch Rate (deg/s)	0	0
Elevator Deflection (deg)	-	-0.1153
Throttle Setting	-	0. 3292

3.3.1 Simulations for the Case 1: Without Disturbance

This section includes the results of the simulations performed for the nominal model, i.e. without any disturbances effect, both for the pure SDRE method and SDRE based SMC (ASMC) method. For comparison purposes, the results for each state variable and control input obtained by two different methods are given together.

The system state variables velocity, flight path angle, altitude, angle of attack and pitch rate are presented in Figures 3.2 to 3.6 respectively while the control inputs, elevator deflection and throttle setting are presented in Figure 3.7 and Figure 3.8.

Figures 3.9 to Figure 3.13 are given to show the variation of the parameters specific to SMC method such as the sigma function, sliding surface slope and the offset of sliding surface from the state space origin. The variation of the sigma function defined in Equation (2.54) is presented Figure 3.9; the offset of sliding surface from the state space origin is presented in Figure 3.10, the components of the sliding surface slope are given in Figure 3.11, Figure 3.12 and Figure 3.13.

Finally, the components of the disturbance or in other words the components of the state dependent disturbance vector are presented in Figure 3.14, Figure 3.15 and Figure 3.16. The delta angle of attack which is resulted from the wind effect and defined in Equation (3.65) is also presented in Figure 3.16.

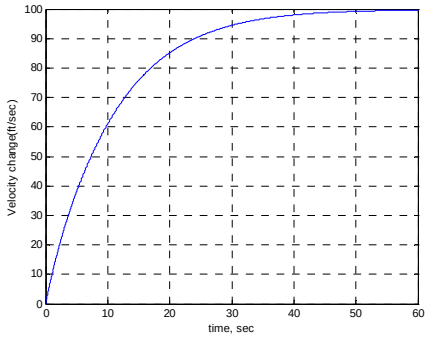

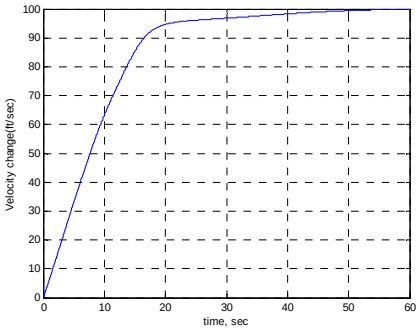

Pure SDRE (LQR) Method SDRE-based SMC Method

Figure 3.2 Velocity Change

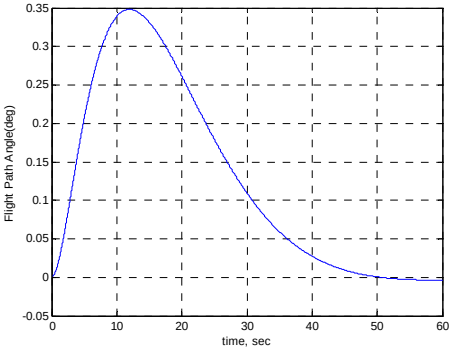

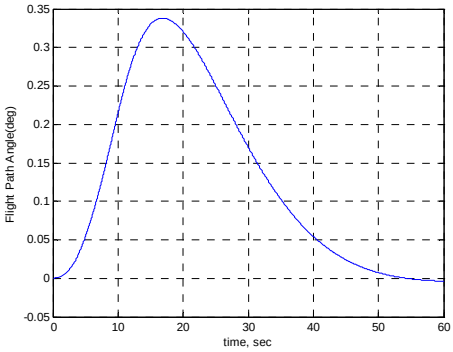

Pure SDRE (LQR) Method SDRE-based SMC Method

Figure 3.3 Flight Path Angle

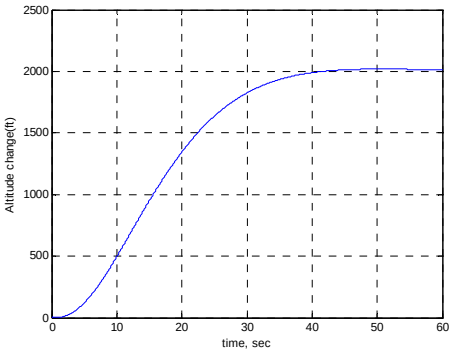

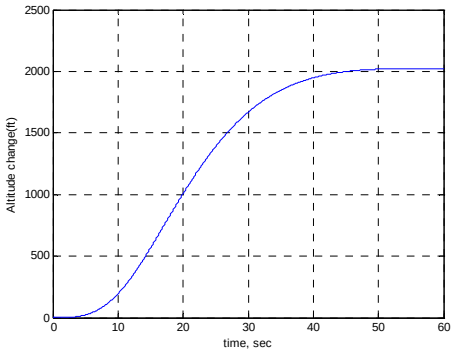

Pure SDRE (LQR) Method SDRE-based SMC Method

Figure 3.4 Altitude Change

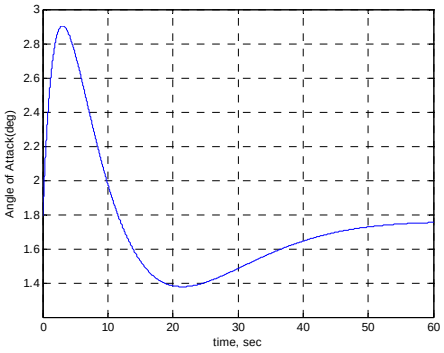

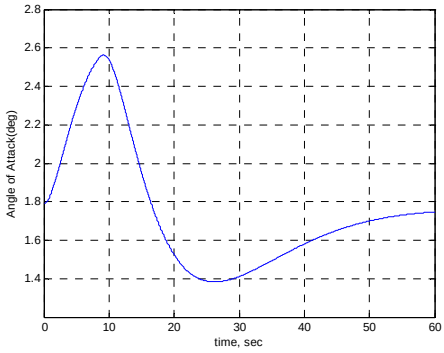

Pure SDRE (LQR) Method SDRE-based SMC Method

Figure 3.5 Angle of Attack

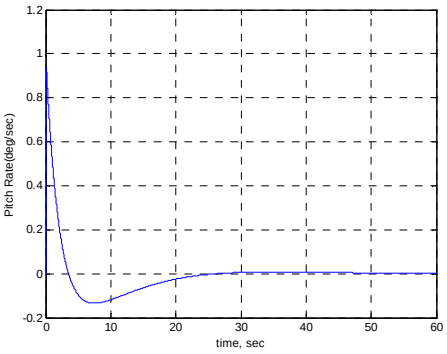

Pure SDRE (LQR) Method

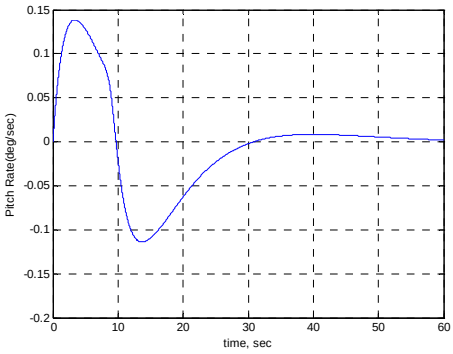

SDRE-based SMC Method

Figure 3.6 Pitch Rate

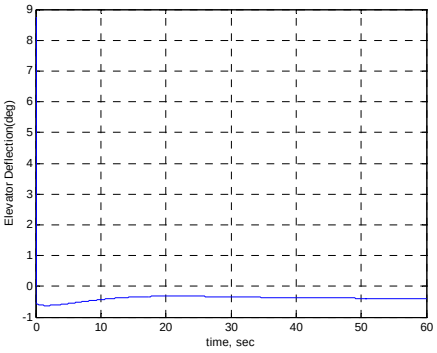

Pure SDRE (LQR) Method

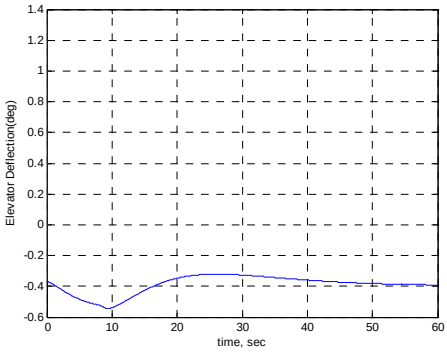

SDRE-based SMC Method

Figure 3.7 Elevator Deflection

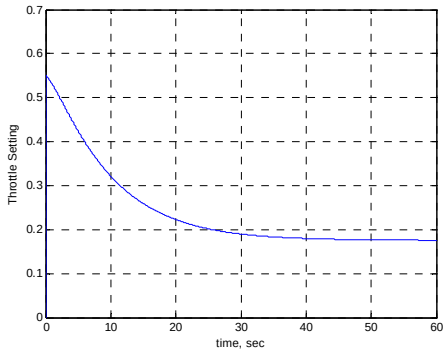

Pure SDRE (LQR) Method

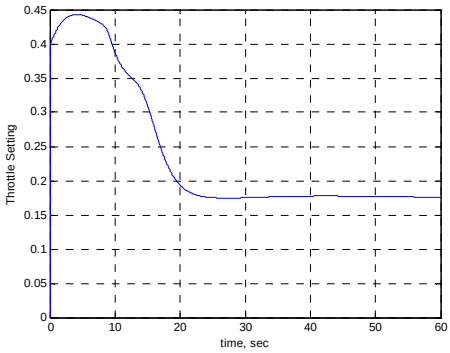

SDRE-based SMC Method

Figure 3.8 Throttle Setting

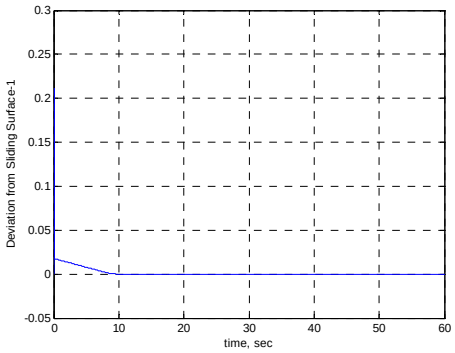

First Component

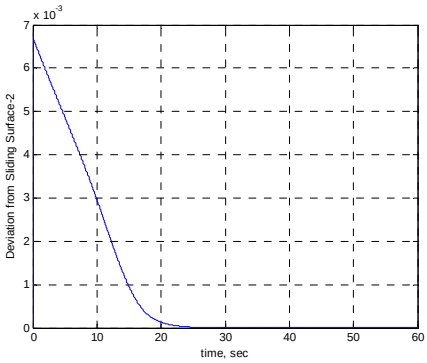

Second Component

Figure 3.9 Variation of the Sigma Function – Deviation from Sliding Surface

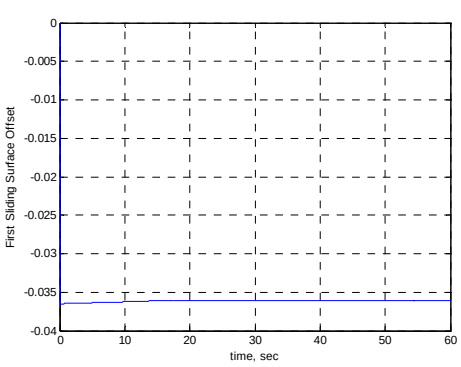

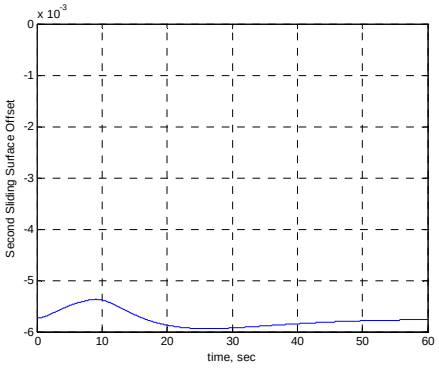

First Component Second Component

Figure 3.10 First and Second Sliding Surface Offset

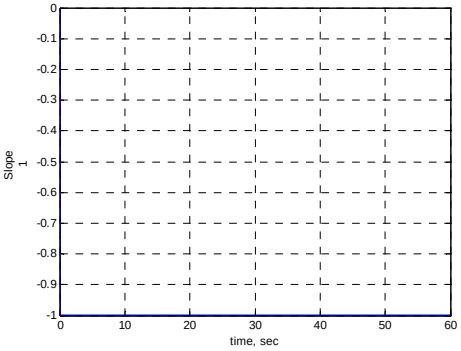

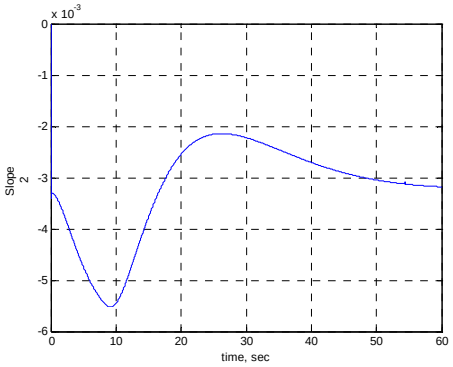

First Component Second Component

Figure 3.11 First and Second Components of the Sliding Surface Slope

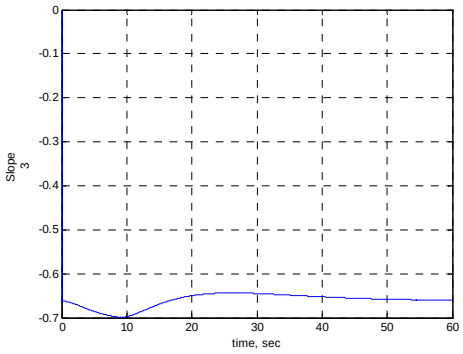

Third Component

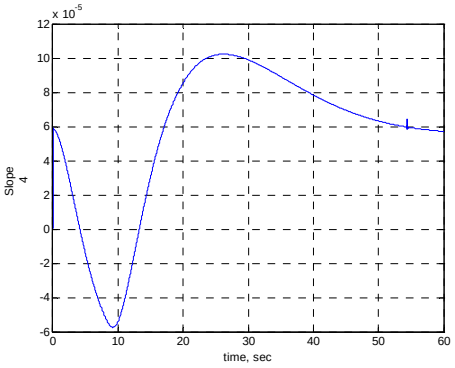

Fourth Component

Figure 3.12 Third and Fourth Components of the Sliding Surface Slope

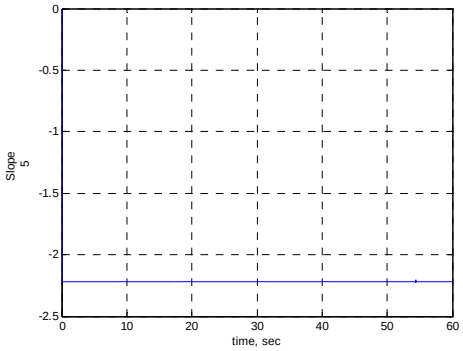

Fifth Component

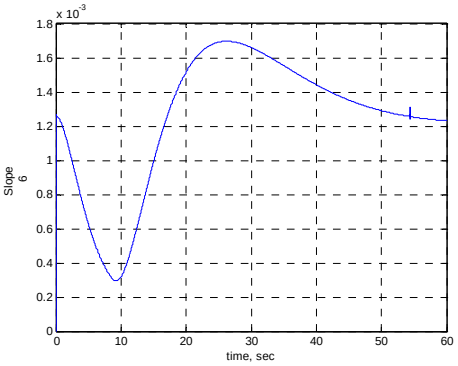

Sixth Component

Figure 3.13 Fifth and Sixth Components of the Sliding Surface Slope

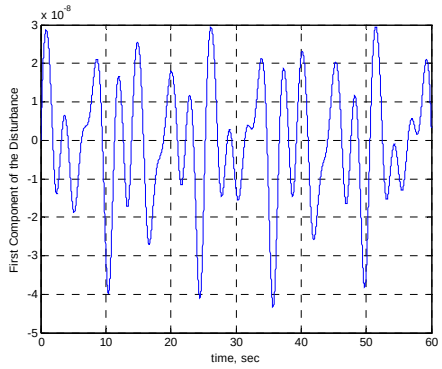

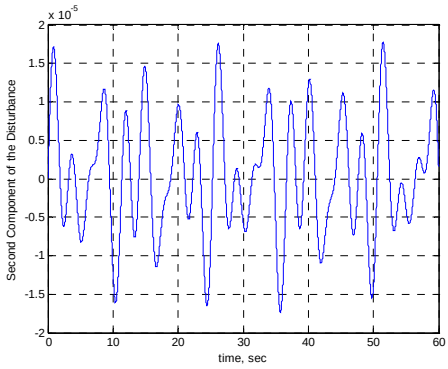

First Component Second Component

Figure 3.14 First and Second Components of the Disturbance

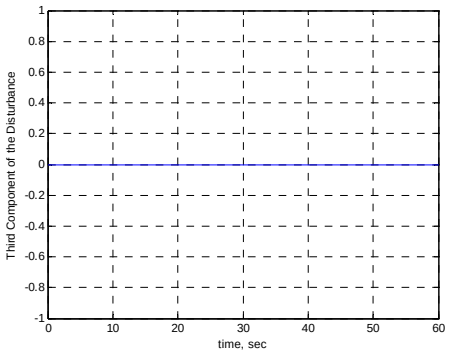

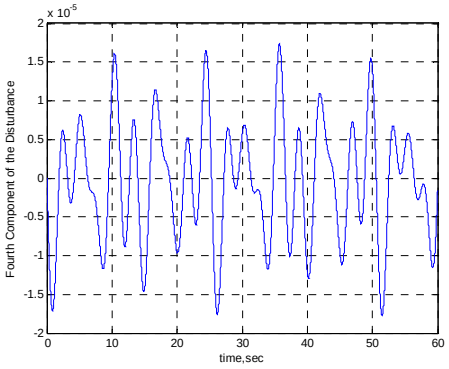

Third Component Fourth Component

Figure 3.15 Third and Fourth Components of the Disturbance

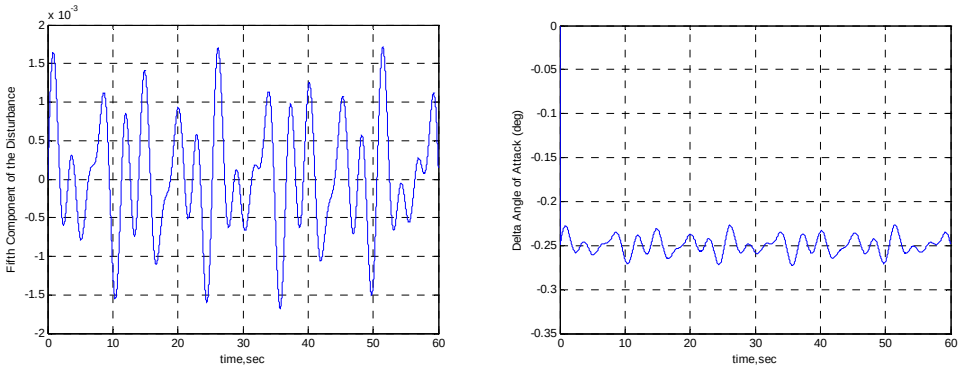

Fifth Component Delta Angle of Attack

Figure 3.16 Fifth Component of the Disturbance and Delta Angle of Attack

3.3.2 Simulations for the Case 2: With Disturbance

This section includes the results of the simulations performed for the model under the presence of disturbance, both for the pure SDRE method and SDRE based SMC (ASMC) method. For comparison purposes, the results for each state variable and control input obtained by two different methods are given together.

The system state variables velocity, flight path angle, altitude, angle of attack and pitch rate are presented in Figures 3.17 to 3.21 respectively while the control inputs, elevator deflection and throttle setting are presented in Figure 3.22 and Figure 3.23.

Figures 3.24 to Figure 3.28 are given to show the variation of the parameters specific to SMC method such as the sigma function, sliding surface slope and the offset of sliding surface from the state space origin. The variation of the sigma function defined in Equation (2.54) is presented Figure 3.24; the offset of sliding surface from the state space origin is presented in Figure 3.25, the components of the sliding surface slope are given in Figure 3.26, Figure 3.27 and Figure 3.28.

Finally, the components of the transformed disturbance or in other words the components of the transformed state dependent disturbance vector are presented in Figure 3.29, Figure 3.30 and Figure 3.31. The delta angle of attack which is resulted from the wind effect and defined in Equation (3.65) is also presented in Figure 3.31.

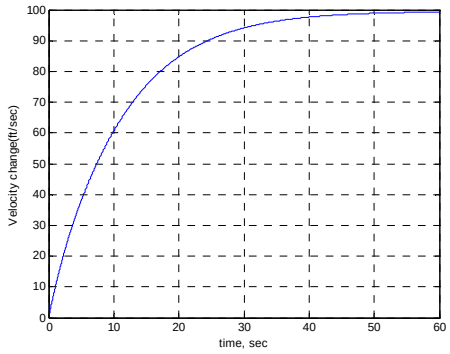

Pure SDRE (LQR) Method

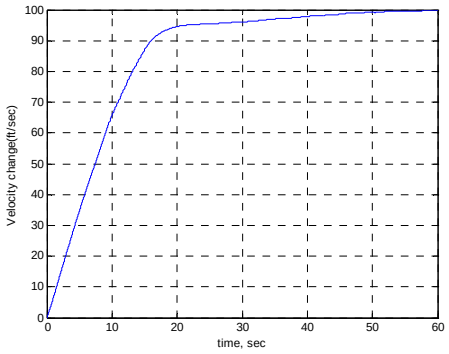

SDRE-based SMC Method

Figure 3.17 Velocity Change

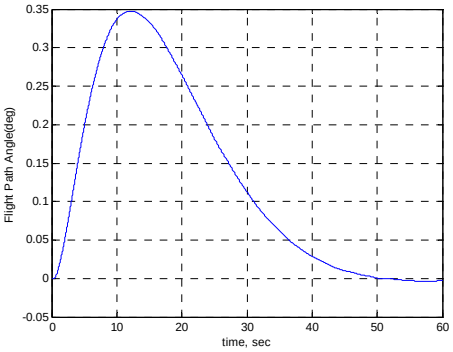

Pure SDRE (LQR) Method

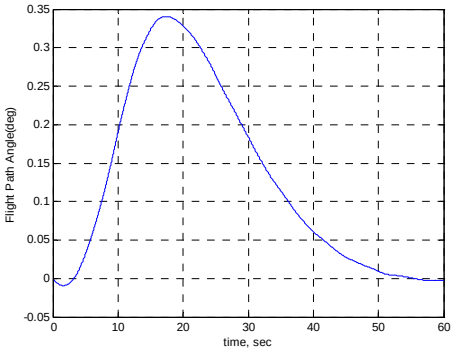

SDRE-based SMC Method

Figure 3.18 Flight Path Angle

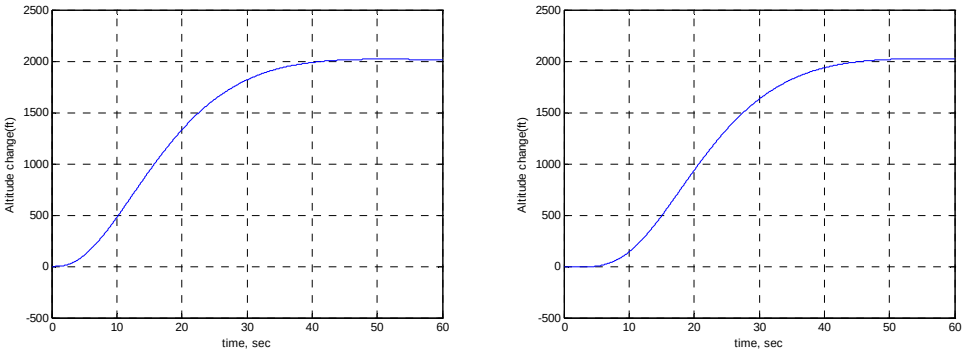

Pure SDRE (LQR) Method SDRE-based SMC Method

Figure 3.19 Altitude Change

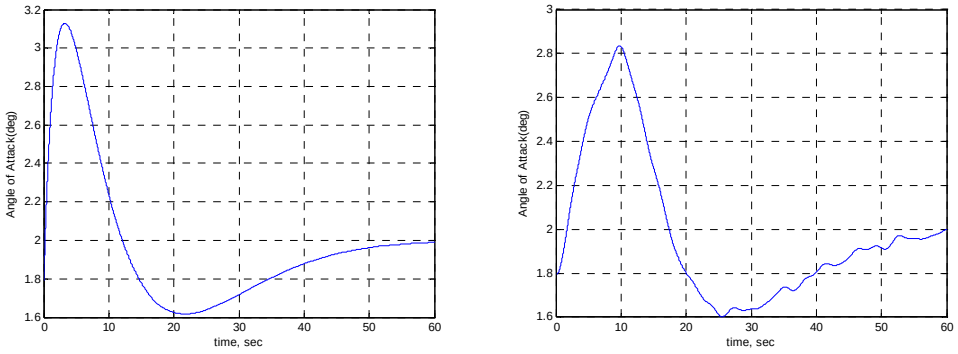

Pure SDRE (LQR) Method SDRE-based SMC Method

Figure 3.20 Angle of Attack

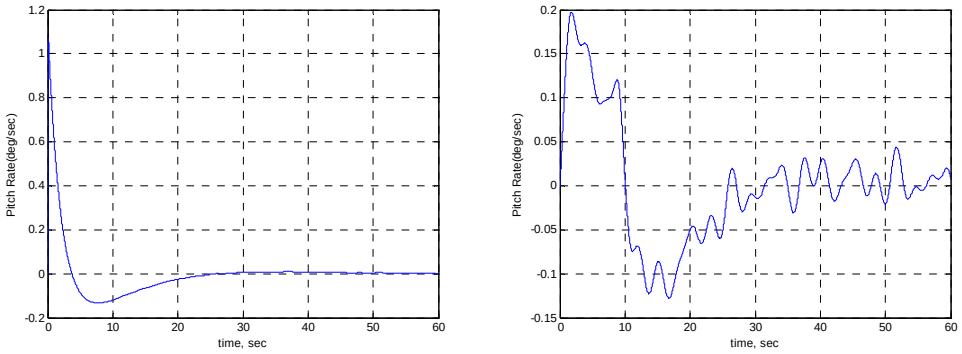

Pure SDRE (LQR) Method SDRE-based SMC Method

Figure 3.21 Pitch Rate

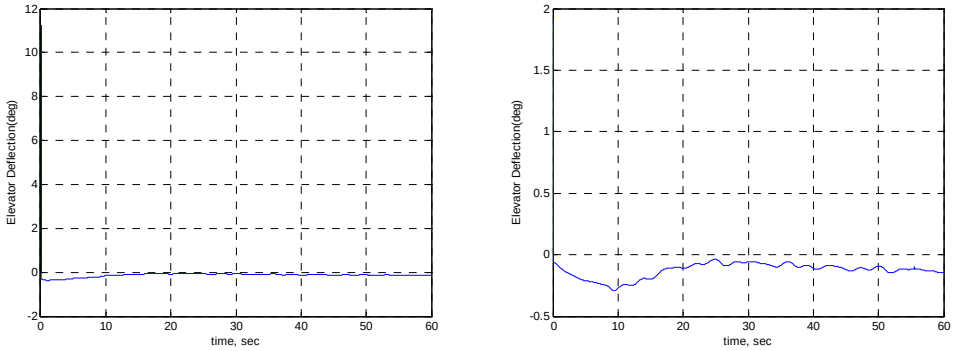

Pure SDRE (LQR) Method SDRE-based SMC Method

Figure 3.22 Elevator Deflection

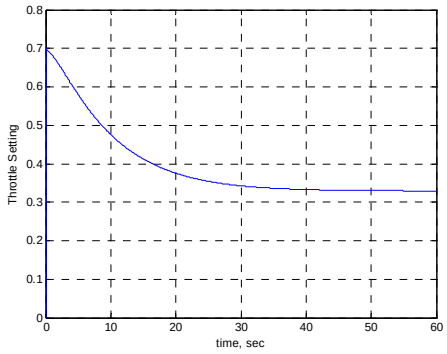

Pure SDRE (LQR) Method

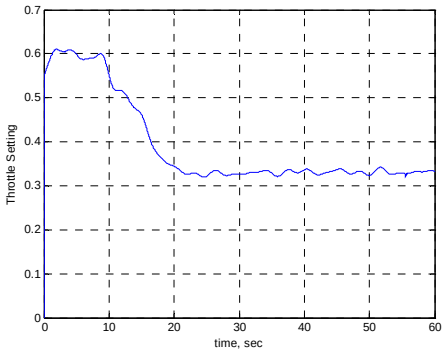

SDRE-based SMC Method

Figure 3.23 Throttle Setting

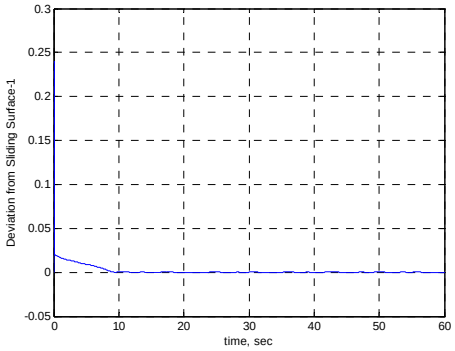

First Component

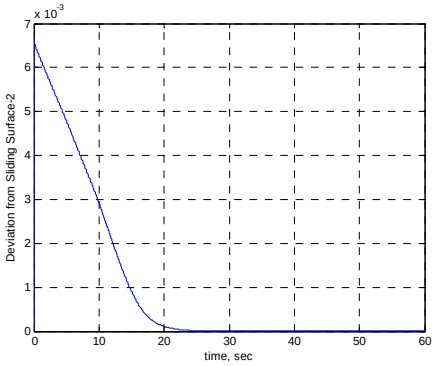

Second Component

Figure 3.24 Variation of the Sigma Function – Deviation from Sliding Surface

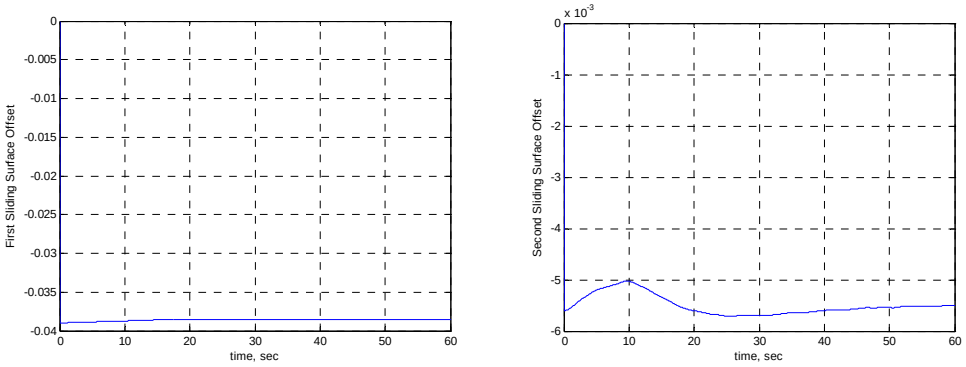

First Component Second Component

Figure 3.25 First and Second Sliding Surface Offset

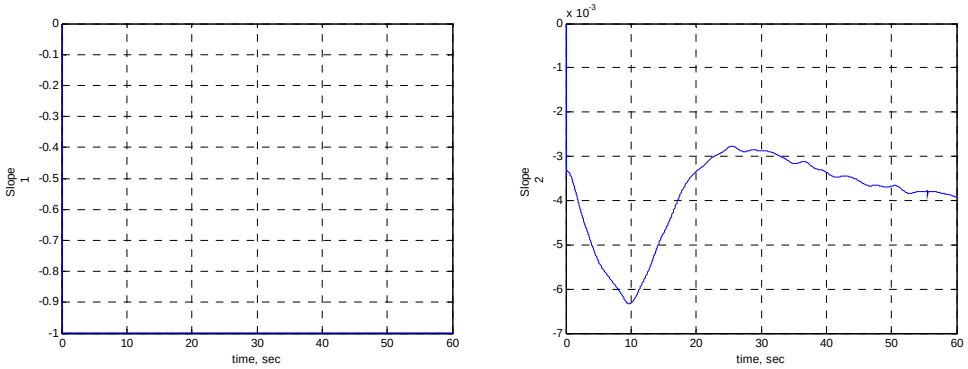

First Component Second Component

Figure 3.26 First and Second Components of the Sliding Surface Slope

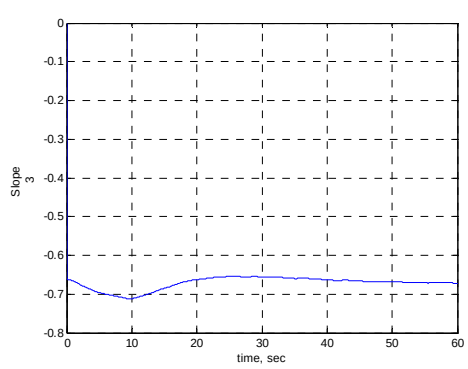

Third Component

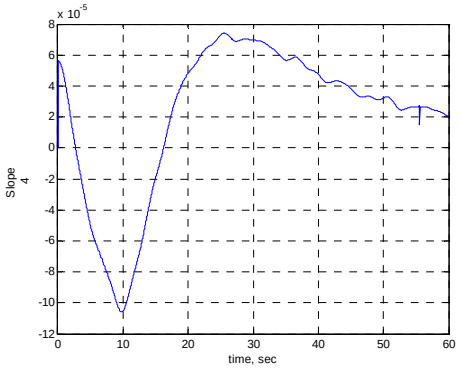

Fourth Component

Figure 3.27 Third and Fourth Components of the Sliding Surface Slope

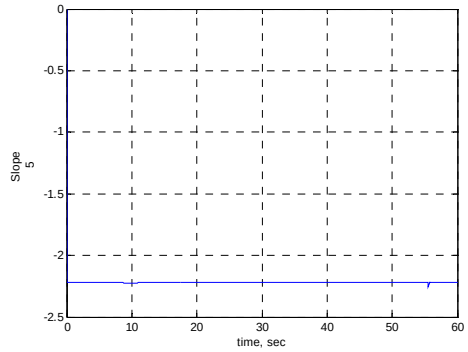

Fifth Component

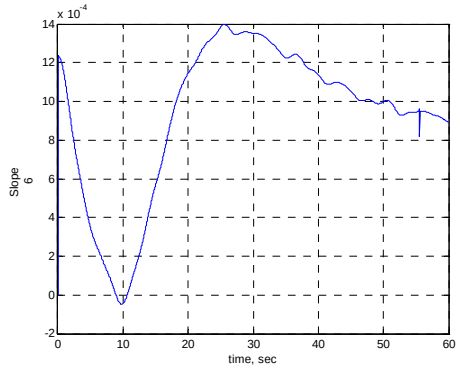

Sixth Component

Figure 3.28 Fifth and Sixth Components of the Sliding Surface Slope

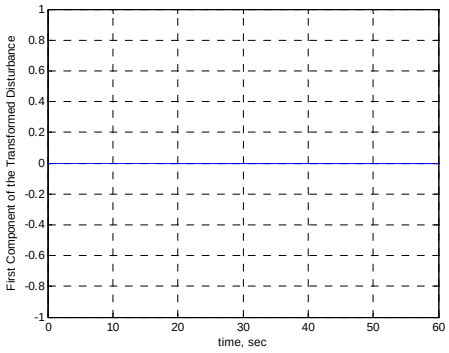

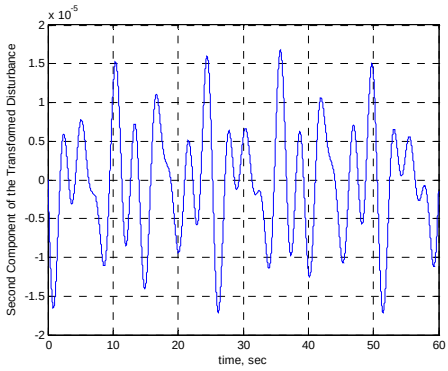

First Component Second Component

Figure 3.29 First and Second Components of the Transformed Disturbance

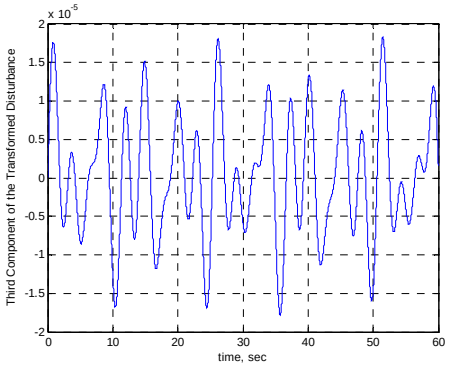

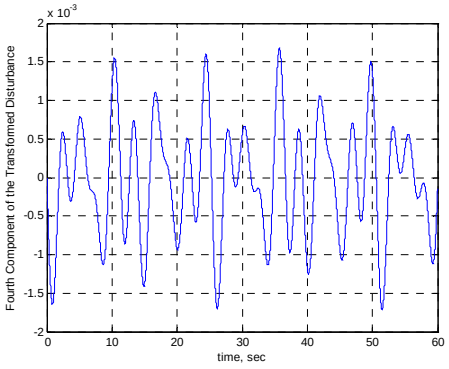

Third Component Fourth Component

Figure 3.30 Third and Fourth Components of the Transformed Disturbance

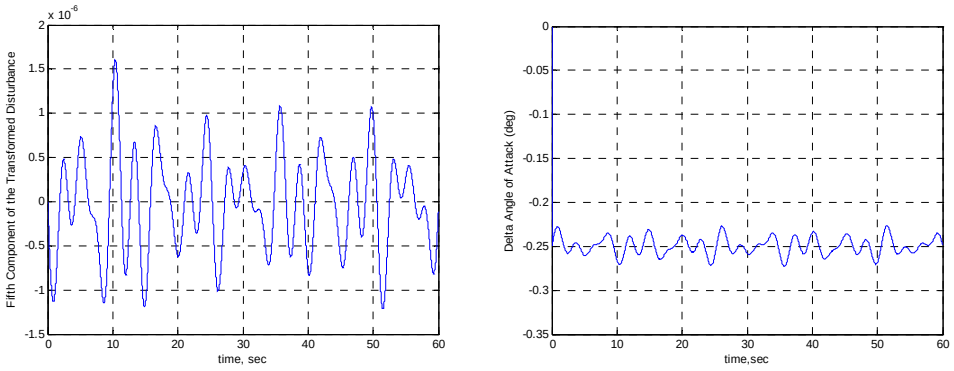

Fifth Component Delta Angle of Attack

Figure 3.31 Fifth Component of the Transformed Disturbance and Delta Angle of Attack

As it can be seen from above figures, simulations have been performed for four cases;

- Pure SDRE (LQR) method applied alone for the nominal model,
- Pure SDRE (LQR) method applied for the model under the presence of disturbance,
- SDRE (LQR) method combined with SMC technique for the nominal model,
- SDRE (LQR) method combined with SMC technique for the model under the presence of disturbance.

It is possible to tune the reaching time to sliding surface, i.e., time needed to reach the steady state conditions and control system performance (values of system state variables and control inputs) by changing the values of **K**, $\mathbf{Q_{11}}$ and $\mathbf{Q_{22}}$.

The proper **K** is to be selected such that the sliding surface is reached in a minimum time and disturbance rejection is maintained simultaneously without destroying the system stability. On the other hand, appropriate $\mathbf{Q_{11}}$ and $\mathbf{Q_{22}}$ matrices should be selected to provide both optimal control effort and feasible controlled system response. For instance, the physical limitations in the state variables such as Angle of Attack and the physical limitations in the control inputs such as the elevator deflection have to be respected. These are the challenging goals of the controller design.

Another point is the effect of using MATLAB® (The MathWorks Inc., 2004) "ode" function. The use of this function very often leads to some perturbations on the system response. One way to handle this problem is to select the integration time step smaller to prevent any numerical error. However, using smaller integration time step increases the simulation time.

It is noted that the relation between integration time step and chattering frequency should be carefully analyzed such that chattering frequency can be caught by integration time step. Since incorrect selection of integration time step may result with erroneous simulation results. In this study, by trial and error method, it is observed that the selected integration time step is sufficient enough to catch the chattering frequency. Here are four examples from case study simulation results which are performed by the use "sign" function to emphasise the effects of incorrect integration time step selection on chattering frequency and results consequently. Control inputs in the case study, elevator deflection and throttle setting are presented for four different integration time step selections. The integration time step is 0.1 for the result presented in Figure 3.32, 0.01 for the result presented in Figure 3.33, 0.001 for the result presented in Figure 3.34 and 0.5 for the result presented in Figure 3.35.

It is concluded that the chattering cannot be observed correctly for the cases given in Figure 3.32 and Figure3.35 while it can be observed correctly for the cases given in Figure 3.33 and Figure 3.34. Therefore, the values 0.01 and 0.01 are determined as good candidates for the integration time step selection.

However, the required time for the simulation increases significantly if the integration time step is selected 0.001 instead of 0.01 and a few numerical errors are observed as seen in Figure 3.34. In summary, 0.01 is selected as an integration time step value for the case study simulations given in section 3.3.1 and 3.3.2.

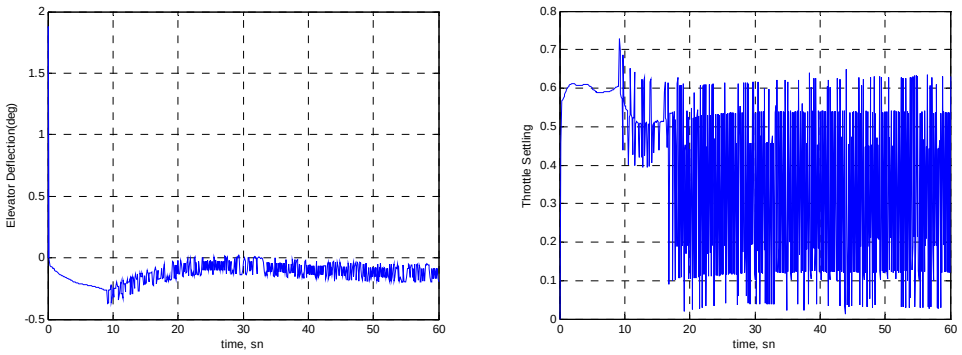

Elevator Deflection Throttle Setting

Figure 3.32 Control Inputs for Integration Time Step is 0.1

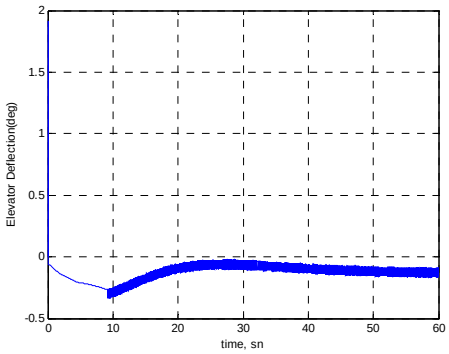

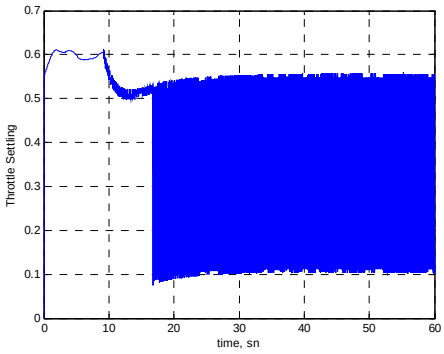

Elevator Deflection Throttle Setting

Figure 3.33 Control Inputs for Integration Time Step is 0.01

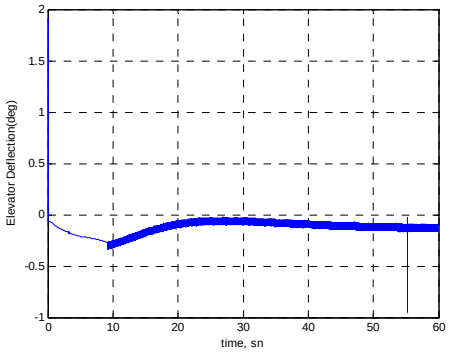

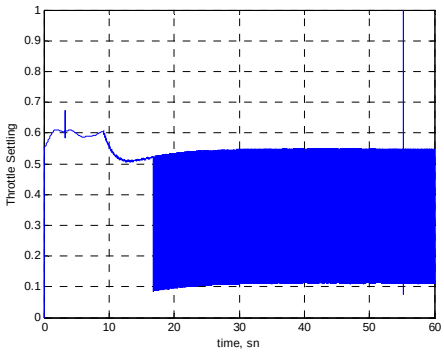

Elevator Deflection Throttle Setting

Figure 3.34 Control Inputs for Integration Time Step is 0.001

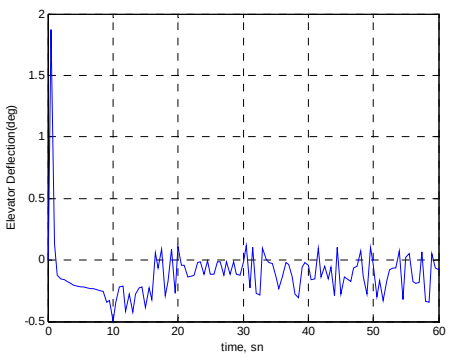

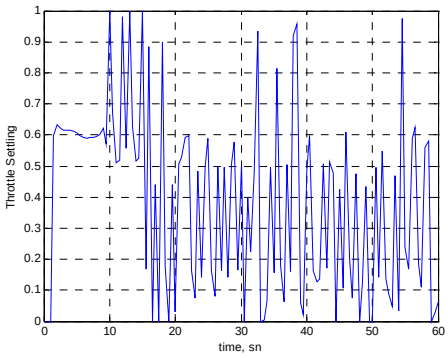

Elevator Deflection Throttle Setting

Figure 3.35 Control Inputs for Integration Time Step is 0.5

The sliding surface slope and the offset of sliding surface from the state space origin are changing with the variations in system state variables and become constant after system state variables had reached their steady state values as expected. This showed that the sliding surface slope and the offset of sliding surface from the state space origin have been adapted for the changes in system state variables (adaptive manner) and the determination of sliding surface slope is optimally selected for the given $\mathbf{Q_{11}}$ and $\mathbf{Q_{22}}$ matrices (optimality manner).

As a summary, proposed SMC is capable of leading the non-linear system up to its desired equilibrium points even under the presence of disturbance.

CHAPTER

4. CONCLUSIONS

4.1 Summary

The aim of this thesis study is to design a sliding mode controller for a linearly actuated non-linear system. A longitudinal model of a generic hypersonic air vehicle is used to show the performance of the proposed controller. The problem can be summarised as tracking the velocity and altitude commands via controlling the deflection of the elevator and thrust by means of a throttle setting both for the nominal model and for the model under the presence of disturbance.

In the first part of the study, brief information about the general SMC design principles and detailed description of the SMC design methodology proposed in this study are given. Then the hypersonic air vehicle model which was studied previously in some papers and the differential equations of the system are presented. In the next chapter, the proposed SMC is derived for this hypersonic air vehicle model based on the principles explained in section 2.2. Finally, simulations are performed on MATLAB® for four cases to observe the controller performance.

4.2 Major Conclusions

The main contribution of this study is to design sliding mode control for a non-linear system by means of solving SDRE's online during the control process and designing the sliding surface correspondingly. This approach both adds an adaptive manner to the classical SMC while combining it with the optimal sliding surface parameter selection.

Adaptive manner includes only the automatic adaptation of the sliding surface by determining the sliding surface slop and the offset of sliding surface from the state space while system state variables are changing.

The method developed in this thesis study is applied to a non-linear flight dynamics which was studied in [10] as well. In [10], another adaptive sliding mode control design approach is suggested. This method is based on the Input-Output linearization technique which requires additional computations. Nonetheless, linearization is made over the nominal model while the original system is still non-linear. This means that the system that was worked on through the controller design phase includes certain amount of approximations beyond linearization.

On the other hand, in this study, a different approach to the SMC is presented which is combined with SDRE. First of all, the system is not linearised to design the sliding mode controller, in other words, the non-linearity of the original system is kept during the controller design phase. Secondly the method computes the required control in a systematic way since it uses the well-known linear quadratic regulator (LQR) algorithms which are available in many existing software.

Not only the practical property of the suggested method in this study, but also the simulation results have some positive features compared to the results of [10]. For instance, in [10], only either velocity or altitude commands are given while in this study, both velocity and altitude commands are given to the same plant and these commands are tracked successfully.

In addition to the above features, the methodology proposed in this study includes some features which can be assumed as relatively new or in other words, which are not common in the literature such as the combining the SDRE technique with the SMC approach and adding the adaptable sliding surface offset term to the definition of the sliding surface.

It is obviously seen from figures that the combined control methodology (ASMC or SMC combined with SDRE) had a basic advantage on the simulations made for nominal model and for the case under the presence of disturbance when compared with the SDRE method. There is a relatively large control effort need for the first method when the performances are compared for both cases. It is a natural outcome of the SMC design technique since SMC is expected to be robust against the disturbances in the input channel (matched disturbances) while SDRE based controller must suppress both matched and unmatched disturbances.

The second reason of this improvement in controller performance is the use of ASMC instead of classic SMC since pure SMC presents drawbacks that include large control authority requirements and chattering. However, the control gains cannot be chosen arbitrary large due to practical considerations such as reaching control surface deflection limits.

Furthermore, control chattering is undesirable in practice because it involves high control activity and may excite high-frequency un-modelled dynamics. These drawbacks are addressed by the addition of adaptation capability to SMC.

4.3 Recommendations for Future Work

As an extension of this thesis study, performance of the proposed ASMC (SDRE combined SMC) can be compared with,

- the SMC designed for the model linearised about the initial and/or final conditions,

- the SMC designed with constant sliding surface parameters, i.e. sliding surface slope and the offset of sliding surface from the state space,

- the pure SDRE method proposed in this study for the cases when there is disturbance with non-zero mean values,

- the pure SDRE method proposed in this study when there are variations in the parameters.

REFERENCES

[1] V. I. Utkin, 1977, *Variable Structure Systems with Sliding Modes*, IEEE Transactions on Automatic Control, 22, pp. 212-222.

[2] C. Edwards, 1998, S. K. Spurgeon, *Sliding Mode Control: Theory and Applications*, Taylor and Francis Ltd.

[3] R.A. De Carlo, S. H. Zak, and G. P. Matthews, 1988, *Variable Structure Control of Nonlinear Multivariable Systems: A Tutorial*, Proceedings of the IEEE, 76, pp. 212-232.

[4] V. I. Utkin, 1992, *Sliding Modes in Control and Optimization,* Berlin: Springer-Verlag.

[5] S. J. Dodds and A. G. Luk'yanov, 1996, *Sliding Mode Block Control of Uncertain Nonlinear Plants*, 13th IFAC Triennial World Congress, pp. 241-146.

[6] H. Sira Ramirez, 1993, *A Dynamical Variable Structure Control Strategy in Asymptotic Output Tracking Problems*, IEEE Transactions on Automatic Control, 38, pp. 615-620.

[7] R. Hirschorn, 2003, *Sliding Mode Control Design for Nonlinear Systems*, Canada Natural Sciences and Engineering Research Council Report.

[8] Y. Niu, J. Lam, X. Wang and D.W.C Ho, 2004, *Observer-based Sliding Mode Control for Nonlinear State-delayed Systems*, International Journal of Systems Science, 35, pp. 139-150.

[9] K. D. Young, V. I. Utkin, Ü. Özgüner, 1999, *A Control Engineer's Guide to Sliding Mode Control*, IEEE Transactions on Control Systems Technology, 7, pp. 328-342.

[10] H. Xu, P. A. Ioannou and M. Mirmirani, *Adaptive Sliding Mode Control Design for A Hypersonic Flight Vehicle*, Journal of Guidance, Control, and Dynamics 2004, vol.27 no.5, pp. 829-838.

[11] J.-J. Slotine, and L. Weiping, 1991, *Applied Nonlinear Control*, Prentice Hall.

[12] C. I. Marrison and R. F. Stengel, , 1998, *Design of Robust Control System For a Hypersonic Aircraft*, Journal of Guidance, Control, and Dynamics, Vol. 21, No. 1.

[13] Q. Wang and R. F. Stengel, 2000, *Robust Nonlinear Control of a Hypersonic Aircraft*, J. of Guidance, Control and Dynamics, Vol. 23, No. 4.

[14] ADEX, S.L., 2007, *Adaptive Predictive Expert Control*, http://www.adexcop.com, 30th of October 2009.

[15] Mracek C. P. and Cloutier J. R., 1998, *Control Designs for the Nonlinear Benchmark Problem via the State-Dependent Riccati Equation Method*, International Journal of Robust And Nonlinear Control, Int. J. Robust Nonlinear Control Vol. 8, pp. 401-433.

[16] M Qian, 1997, *Sliding Mode Controller Design for ABS System*, M.Sc. Thesis, Electrical and Computer Engineering Department, College of Natural Resources, Virginia Tech.

[17] Utkin, V.I. and Young, K.-K.D, 1978, *Methods for Constructing Discontinuity Planes in Multidimensional Variable Structure Systems*, Automation and Remote Control Vol. 39, pp. 1466-1470.

[18] Banks, S.P., Salamcı, M.U. and Özgören, M.K., 1999, *On the Global Stabilization of Nonlinear Systems via Switching Manifolds*, Turk J Elec Engin, Vol.7, No.1-3 © TUBITAK.

[19] İtik M., Salamcı, M.U. and Ülker F. D., 2005, Vibration Suppression of An Elastic Beam via Sliding Mode Control, E. Inan and A. Kırış (eds), Vibration Problems ICOVP 2005, pp. 237–242 © 2007 Springer.

[20] Itik M., Salamcı, M.U., Ülker F. D. and Yaman, Y., 2005, *Active Vibration Suppression of a Flexible Beam via Sliding Mode and H∞ Control*, Decision and Control, 2005 and 2005 European Control Conference, pp. 1240-1245.

[21] Itik M., Salamcı, M.U. and Banks, S.P., 2009, *Optimal Control Of Drug Therapy In Cancer Treatment*, Nonlinear Analysis: Theory, Methods & Applications, in Press.

[22] Tombul G. S., Banks S. P.,and Akturk N., 2009, *Sliding Mode Control For A Class Of Non-Affine Nonlinear Systems* , Nonlinear Analysis: Theory, Methods & Applications, in Press, Corrected Proof.

[23] Salamcı, M.U., Özgören, M.K. and Banks, S.P., 2000, *Sliding Mode Control with Optimal Sliding Surfaces for Missile Autopilot Design*, Journal of Guidance, Control, And Dynamics, Vol. 23, No. 4.

[24] Salamcı, M.U. and Gökbilen B., 2007, *SDRE Missile Autopilot Design using Sliding Mode Control with Moving Sliding Surfaces*, 17th IFAC Symposium on Automatic Control in Aerospace.

[25] Salamcı, M.U. and Gökbilen B., 2006, *Doğrusal Olmayan Sistemlerin Zamanla Değişen Doğrusal Yüzey Kullanılarak Kayan Kipli Kontrolü ve Uygulamaları*, M.Sc. Thesis, Mechanical Engineering Department, Gazi University.

[26] Salamcı, M.U. and Gökbilen B., 2006, *Alçak Yörüngeli Küçük Uyduların Doğrusal Olmayan Konum Kontrolü, Otomatik Kontrol Ulusal Toplantısı*, TOK'06, TOBB Ekonomi ve Teknoloji Üniversitesi.

[27] Salamcı, M.U. and Tombul G. S., 2006, *Sliding Mode Control Design with Time Varying Sliding Surfaces for a Class of Nonlinear Systems*, Proceedings of the 2006 IEEE, International Conference on Control Applications.

[28] Çimen T., 2008, *State-Dependent Riccati Equation (SDRE) Control: A Survey*, Proceedings of the 17th World Congress, The International Federation of Automatic Control.

[29] Wang Y.-P. and Sinha A., 1998, *Adaptive Sliding Mode Control Algorithm for a Microgravity Isolation System*, Acta Astronautica, Vol. 43, No. 7-8, pp. 377-384.

[30] Yau H.-T. and Yan J.-J., 2008, *Adaptive Sliding Mode Control of a High-Precision Ball-Screw-Driven Stage*, Nonlinear Analysis: Real World Applications.

[31] Huang Y.-J., Kuo T.-C. and Chang S.-H., 2008, *Adaptive Sliding-Mode Control for Nonlinear Systems With Uncertain Parameters*, IEEE Transactions On Systems, Man, And Cybernetics - Part B: Cybernetics, Vol. 38, No. 2.

[32] Huang A.-C. and Chen Y.-C., 2004, *Adaptive Sliding Control for Single-Link Flexible-Joint Robot With Mismatched Uncertainties*, IEEE Transactions on Control Systems Technology, Vol. 12, No. 5.

[33] Yoerger D. R. and Slotine J.-J. E., 1991, *Adaptive Sliding Control of an Experimental Underwater Vehicle*, Proceedings of the 1991 IEEE International Conference on Robotics and Automation.

[34] Wai R.-J., 2000, *Adaptive Sliding Mode Control for Induction Servomotor Drive*, IEE Pwc.-Cleclr. Power Appl,, Vol. 147, No. 6.

[35] D Zhou, Mu, C. and Xu W., 1999, *Adaptive Sliding-Mode Guidance of a Homing Missile*, Journal of Guidance, Control, and Dynamics, Vol. 22, No. 4.

[36] Lee K. W., Nambisan P. R. And Singh S. N., 2008, *Adaptive Variable Structure Control of Aircraft with an Unknown High-Frequency Gain Matrix*, Journal of Guidance, Control, and Dynamics, Vol. 31, No. 1.

[37] H.K. Khalil, 1996, *Nonlinear Systems,* New Jersey: Printice-Hall.

[38] Cloutier J. R., 1997, *State-Dependent Riccati Equation Techniques: An Overview*, Proceedings of the American Control Conference Albuquerque.

[39] Erdem E. B. and Alleyne A. G., 2004, *Design of a Class of Nonlinear Controllers via State Dependent Riccati Equations*, IEEE Transactions on Control Systems Technology, Vol. 12, No. 1.

[40] Diong B. M., 2004, *Sliding Mode Control Design for a Class of Systems With Non-Matching Nonlinearities and Disturbances*, International Journal of Systems Science, Volume 35, Number 8, 10 July 2004, pp. 445–455.

[41] Kim K.-S., Park Y. and Oh S.-H., 2000, *Designing Robust Sliding Hyperplanes for Parametric Uncertain Systems: a Riccati Appr*oach, Automatica No.36, pp. 1041 - 1048.

[42] Spurgeon S. K. and Lu X. Y., 1997, *Output Tracking Using Dynamic Sliding Mode Techniques*, International Journal of Robust and Nonlinear Control, Vol. 7, pp. 407 – 427.

[43] Chou C.-H. and Cheng C.-C., 2001, *Design of Adaptive Variable Structure Controllers for Perturbed Time-Varying State Delay Systems*, Journal of the Franklin Institute, Vol. 338, pp. 35 – 46.

APPENDIX A

MAIN SCRIPT

```
clc;clear;
tic
global t_inc k tspan xd ud

epsilonbig=1e-6;
epsilonsml=1e-9;

xd=[15160;
   0;
   112000;
   2.00042687579048*pi/180;
   0];

ud=[-0.11534710655337*pi/180;0.32921240198018];

x0(1)=15060;
x0(2)=(0+epsilonsml)*pi/180;
x0(3)=110000;
x0(4)=1.79*pi/180;
x0(5)=(0+epsilonsml)*pi/180;
```

```
x0(1)=(0)/(15060);
x0(3)=(0)/(110000);
xd(1)=(100)/(15060);
xd(3)=(2000)/(110000);

format long;
xtilde=x0;


t_start=0;        % Starting time
t_final=60;       % Final time
t_inc=1e-2;       % Time increment value
tspan=[t_start:t_inc:t_final];

k=[-0.002 -0.0004];
k=diag(k);% factor that maintains the sliding direction is shifted to zero


%-------------------------------------------------------------------------%
% ODE Solver
%-------------------------------------------------------------------------%
display('Solution is running');
[x,Ucon,sigma,KY,h2,d2]=ode5x(@control,tspan,xtilde);
      result(1).x1=(15060*(x(:,1)+1))-15060;
      result(1).x2=180/pi*(x(:,2));
      result(1).x3=(110000*(x(:,3)+1))-110000;
      result(1).x4=180/pi*(x(:,4));
      result(1).x5=180/pi*(x(:,5));
      result(1).U1=180/pi*(Ucon(1,:));
      result(1).U2=(Ucon(2,:));
      result(1).sigma1=sigma(1,:);
      result(1).sigma2=sigma(2,:);
```

```
    hh2=cell2mat(h2);
    result(1).h21=hh2(1,:);
    result(1).h22=hh2(2,:);
    dd2=cell2mat(d2);
    result(1).d21=dd2(1,:);
    result(1).d22=dd2(2,:);
    result(1).time=tspan;

% C hesaplama ve plot
for i=1:6

  for j=1:length(KY)
    C(i,j)=KY{j}(i);
  end
  figure(i+13); plot (tspan,C(i,:)),xlabel('time, sn'),ylabel({'Slope ', i}); grid on;
end

%%

figure (1); plot (result(1).time,result(1).x1),xlabel('time, sn'),ylabel('Velocity
change(ft/sec)'); grid on;
figure (2); plot (result(1).time,result(1).x2),xlabel('time, sn'),ylabel('Flight Path
Angle(deg)'); grid on;
figure (3); plot (result(1).time,result(1).x3),xlabel('time, sn'),ylabel('Altitude
change(ft)'); grid on;
figure (4); plot (result(1).time,result(1).x4),xlabel('time, sn'),ylabel('Angle of
Attack(deg)'); grid on;
figure (5); plot (result(1).time,result(1).x5),xlabel('time, sn'),ylabel('Pitch
Rate(deg/sec)'); grid on;
figure (6); plot (result(1).time,result(1).U1),xlabel('time, sn'),ylabel('Elevator
Deflection(deg)'); grid on;
```

```
figure (7); plot (result(1).time,result(1).U2),xlabel('time, sn'),ylabel('Throttle Setting');
grid on;
figure (8); plot (result(1).time,result(1).sigma1),xlabel('time, sn'),ylabel('First Sliding
Surface'); grid on;
figure (9); plot (result(1).time,result(1).sigma2),xlabel('time, sn'),ylabel('Second
Sliding Surface'); grid on;
figure (10); plot (result(1).time,result(1).h21),xlabel('time, sn'),ylabel('First Sliding
Surface Offset'); grid on;
figure (11); plot (result(1).time,result(1).h22),xlabel('time, sn'),ylabel('Second Sliding
Surface Offset'); grid on;
figure (12); plot (result(1).time,result(1).d21),xlabel('time, sn'),ylabel('First
Component of the Disturbance'); grid on;
figure (13); plot (result(1).time,result(1).d22),xlabel('time, sn'),ylabel('Second
Component of the Disturbance'); grid on;

toc
display('Process Finished.');
```

APPENDIX B

FUNCTION FOR DESIGNING CONTROLLER

```
function [phitildedot,Ucon,sigma,C,Tr,h2,d2]=control(t,phitilde,Cp,Tp,h2p)

global t_inc xd ud

   epsilonbig=1e-6;
   epsilonsml=1e-9;

phid=xd;


%% Transformation of the system to Canonical Form

[A,B,F,D] = sistem(phitilde);

Tr=T_find(A,B);

   if (t==0)
      Told=Tr;
   else
      Told=Tp;
   end

Tp=Told;
 Tdot=(Tr-Told)/t_inc;
```

```
[Tr,Abar11,Abar12,Abar21,Abar22,Bbar2]=T_find(A,B,Tdot);

contr=ctrb(Abar11,Abar12);

% rank(contr);
% if(rank(contr)==length(Abar11)) display('Controllable System');
%
% else display('System is Uncontrollable !!!!!!!!!!!!!!!!!');
% end

% ranks=rank(sym(contr));
% if(ranks==length(Abar11)) display('Controllable System');
%
% else display('System is Uncontrollable !!!!!!!!!!!!!!!!!');
% end

%% Determination of Sliding Surface Slope and the Offset of the Sliding Surface
%% Surface

[C h2]=c_find(Abar11,Abar12,phitilde,F,Tr);

   if (t==0)
      Cold=C;
      h2old=h2;
   else
      Cold=Cp;
      h2old=h2p;
   end

% Cp=Cold;
% h2p=h2old;
```

```
Cdot=(C-Cold)/t_inc;  % Time derivative of C matrix Cdot = d(T)/dt
h2dot=(h2-h2old)/t_inc;


%% Sliding Mode Control Design

z=Tr*phitilde;
f=Tr*F;
f1=f(1:3,1);
f2=f(4:5,1);
z1=z(1:3,1);
z2=z(4:5,1);
sigma=C*z1+z2-h2;


%% Disturbance Injection

Im=-0.25*pi/180;
If=0.025*pi/180*(sin(t)+sin((3^0.5)*t)+sin((5^0.5)*t))/3;

D(1)=D(1)*((2*0.645*Im*If)+(0.645*If^2)+(0.0043378*If));

D(2)=D(2)*(0.6203*If);
D(5)=D(5)*((-0.035)*2*Im*If-(0.035*If^2)+0.036617*If);


%% Relation between SMC Gain and Disturbance

g=Tr*D;
d1=g(1:3,1);
d2=g(4:5,1);
```

```
% Equivalent Control

ueq=-inv(Bbar2)*(Cdot*z1+C*(Abar11*z1+Abar12*z2+f1)+...
   (Abar21*z1+Abar22*z2+f2)-h2dot);

 % High Frequency control signal

global k;
uhf=inv(Bbar2)*k*tanh(1000*sigma);...smooth;

Ucon=ueq+uhf;

%% Physical Limitations on Control Inputs

if Ucon(2,:)<0;
   Ucon(2,:)=0;
end

if Ucon(2,:)>1;
   Ucon(2,:)=1;
end

if (180/pi*Ucon(1,:))>1;
   Ucon(1,:)=1*pi/180;
end

 %% Differential Equation

phitildedot=A*phitilde+B*Ucon+F+D;
```

APPENDIX C

FUNCTION FOR CONSTRUCTING SYSTEM AND CONTROL MATRICES

```
function [A,B,F,D]=sistem(x0)
%%-------------------------------------------------------------------------
% This function is to describe the dynamics of the system without an unbalanced
% mass. The only external effect is gravity.
% dx/dt = A(x)*x + B(x,u)*u + F;
% global

epsilonsml=1e-9;

%% Initialisation of the matrices.
%-------------------------------------------------------------------------
A=zeros(5,5);
B=zeros(5,2);
F=zeros(5,1);

% ---------------------------------
% p ve ne degerlerinin belirlenmesi
% ---------------------------------
   p=0;
   n=0.02576;
% % ---------------------------------

Im=-0.25*pi/180;
```

```
%%%%%%%%%
V=15060*(1+x0(1));
gamma=x0(2);
h=110000*(1+x0(3));
alpha=x0(4);
q=x0(5);
%%%%%%%%%

m=9375;
Iyy=7*10^6;
S=3603;
cbar=80;
ce=0.0292;
mu=1.39*10^16;
RE=20903500;
ro=0.24325*1e-4;

r=h+RE;

 a11=-(15060)*(1/15060)*(((ro*V*S/(m))*0.003772));
a12=-(1/15060)*(mu*sin(gamma)/(r^2*(gamma+epsilonsml)));
a14=-(1/15060)*((ro*V^2*S/(2*m))*(0.6450*alpha+0.0043378));
b12=(1/15060)*(((ro*V^2*S/(2*m))*n*cos(alpha)));
%
a21=-(15060)*(((mu-V^2*r)*cos(gamma))/(V^2*r^2));
a24=((ro*V*S/(2*m))*0.6203);
b22=((ro*V*S/(2*m))*n*sin(alpha));

a32=(1/110000)*(V*(sin(gamma)/(gamma+epsilonsml)));

a41=(15060)*(((mu-V^2*r)*cos(gamma))/(V^2*r^2));
a44=-((ro*V*S/(2*m))*0.6203);
```

```
a45=1;
b42=-((ro*V*S/(2*m))*n*sin(alpha));
a51=(15060)*((ro*V*S)*cbar*(5.3261*10^-6)/Iyy);
a54=(0.5*(ro*V^2*S)*cbar*(-ce-
0.035*alpha+0.036617)/Iyy)+(0.25*(ro*V*S*q)*(cbar^2)*(-
6.796*alpha+0.3015)/Iyy);
a55=(0.25*(ro*V*S)*(cbar^2)*(-0.2289)/Iyy);

b51=(0.5*(ro*V^2*S)*cbar*ce/Iyy);

f1=(-(((ro*V*S/(m))*0.003772)))-
(1/15060)*(((ro*V^2*S/(2*m))*(0.645*Im^2+0.0043378*Im)));
f2=(-(15060)*(((mu-
V^2*r)*cos(gamma))/(V^2*r^2)))+(ro*V*S/(2*m))*(0.6203*Im);
f3=0;
f4=(15060)*((((mu-V^2*r)*cos(gamma))/(V^2*r^2)));
f5=((15060)*((ro*V*S)*cbar*(5.3261*10^-6)/Iyy))+((0.5*(ro*V^2*S*cbar)*(-
0.035*Im^2+0.036617*Im)/Iyy));


d1=-(1/15060)*(ro*V^2*S/(2*m));
d2=(ro*V*S/(2*m));
d3=0;
d4=0;
d5=(0.5*(ro*V^2*S*cbar/Iyy));


%%%%%%%%%%
A=[a11 a12 0 a14 0;a21 0 0 a24 0;0 a32 0 0 0;a41 0 0 a44 a45;a51 0 0 a54 a55];
B=[0 b12;0 b22;0 0;0 b42;b51 0];
F=[f1;f2;f3;f4;f5];
D=[d1;d2;d3;d4;d5];
```

APPENDIX D

FUNCTION FOR TRANSFORMING THE SYSTEM TO CANONICAL FORM

```
function [Tr,varargout]=T_find(A,B,varargin)
% Transformation matrix for suitable canonical form. [0;B2]
%       Burak DURMAZ


%-------------------------------------------------------------------------%
% Establish the size of the input distribution matrix
%-------------------------------------------------------------------------%
[nn,mm]=size(B);

%-------------------------------------------------------------------------%
% Perform QR decomposition on the input distribution matrix
%-------------------------------------------------------------------------%
[Tr temp]=qr(B);
Tr=Tr';
Tr=[Tr(mm+1:nn,:);Tr(1:mm,:)];

 if (nargout>1)
   if(nargin>3)
      Tdot=varargin{1};
   else
      Tdot=zeros(nn);
   end
```

```
%-------------------------------------------------------------------------%
% Obtain (Areg,Breg); regular form description
%-------------------------------------------------------------------------%

Areg=Tr*A*Tr'+Tdot*Tr';
Breg=Tr*B;

%-------------------------------------------------------------------------%
% Obtain matrix sub-blocks for sliding mode controller design
%-------------------------------------------------------------------------%

A11 = Areg(1:nn-mm,1:nn-mm);
A12 = Areg(1:nn-mm,nn-mm+1:nn);
A21 = Areg(nn-mm+1:nn,1:nn-mm);
A22 = Areg(nn-mm+1:nn,nn-mm+1:nn);
B2 = Breg(nn-mm+1:nn,1:mm);


varargout{1}=A11;
varargout{2}=A12;
varargout{3}=A21;
varargout{4}=A22;
varargout{5}=B2;

end
```

APPENDIX E

FUNCTION FOR SLIDING SURFACE SLOPE DETERMINATION

```
function [S,varargout]=c_find(A11,A12,phitilde,F,Tr,varargin)
% Sliding Hyperplane Design with LQR method.
%       Burak DURMAZ

global t_inc xd ud

L=zeros(5,2);
[nn,mm]=size(L);

Q=diag([10 1 1 0.2 1])*1e2*3;
Qt=Tr*Q*Tr';

Q11 = Qt(1:nn-mm,1:nn-mm);
Q12 = Qt(1:nn-mm,nn-mm+1:nn);
Q21 = Qt(nn-mm+1:nn,1:nn-mm);
Q22 = Qt(nn-mm+1:nn,nn-mm+1:nn);

% Form reduced order system description and associated weighting matrix
Qhat=Q11;...-Q12*inv(Q22)*Q21;
Ahat=A11;...-A12*inv(Q22)*Q21;

A=Ahat;
B=A12;
Q=Qhat;
R=Q22;
```

```
% Solve the LQR problem
[K,S,E]=lqr(A,B,Q,R);


z=Tr*phitilde;
f=Tr*F;
r=Tr*xd;
f1=f(1:3,1);
f2=f(4:5,1);
z1=z(1:3,1);
z2=z(4:5,1);
r1=r(1:3,1);
r2=r(4:5,1);

G=B*inv(R)*B';
psi=inv(-A'+S*G)*((-Q*r1)+S*(f1+B*r2));
slope=inv(R)*(B')*S;
h2=r2-inv(R)*(B')*psi;

% Obtain the switching function matrix in terms of the original coordinates
S=slope;
varargout{1}=h2;
```

APPENDIX F

BRIEF USER MANUAL

The “Mainscript” is the main baseline of this study’s software coding as it can be understood from its name. It is enough for the user to run this program to see all the results. Since all other functions are automatically called by this main script. The initial and desired values which are related with system state variables and control inputs can be adjusted in main script also. Additional, the gain of the sliding mode controller, k and simulation time adjustments have been changed in main script.

To adjust the weighting matrices Q and R, user can set the Q11 for adjusting Q and Q22 for adjusting R in function “c_find” given in E.

System matrices f and B are constructed in function “sistem” given in C. and all the constant system parameters are also embedded inside this function.

The function “T_find” given in D. is used to transform the system in to the canonical form in order to design the SMC via the proposed method.

The most important function is called “control”, given in B. and it determines the SMC with the help of other functions.

CURRICULUM VITAE

PERSONAL INFORMATION

Surname, Name: Durmaz, Burak
Nationality: Turkish (TC)
Date and Place of Birth: 1 January 1983, Isparta
Marital Status: Single
Phone: + 90 312 811 26 11
Email: bdurmaz@tai.com.tr

EDUCATION

Degree	Institution	Year of Graduation
Double Major Program	Gazi University, Electrical and Electronics Engineering Department	2006
BS	Gazi University, Mechanical Engineering Department	2005
High School	Isparta Süleyman Demirel Fen Lisesi, Isparta	2001

WORK EXPERIENCE

Year	Place	Enrolment
2006-Present	Turkish Aerospace Industries , Inc. (TAI)	Systems Engineer

FOREIGN LANGUAGES

Advanced English, Basic German

PUBLICATIONS

1. Burak D., Mine Alemdaroğlu T., Pınar E. "Tusaş Uçuş/Sistem Emniyeti Faaliyetlerinin Değerlendirilmesi ve Geleceğe Yönelik Öneriler", Savunma Sanayii Müsteşarlığı (SSM) III. Kalite Kurultayı (2008)

HOBBIES
Swimming, History, Politics, Movies, Dance, Football, Travel